Noise-induced unstable dimension variability and transition to chaos in random dynamical systems

Ying-Cheng Lai,[1,2] Zonghua Liu,[1] Lora Billings,[3] and Ira B. Schwartz[4]
[1]*Department of Mathematics, Center for Systems Science and Engineering Research, Arizona State University, Tempe, Arizona 85287*
[2]*Departments of Electrical Engineering and Physics, Arizona State University, Tempe, Arizona 85287*
[3]*Department of Mathematical Sciences, Montclair State University, Upper Montclair, New Jersey 07043*
[4]*Plasma Physics Division, Naval Research Laboratory, Code 6792, Washington, DC 20375*
(Received 29 August 2002; published 19 February 2003)

Results are reported concerning the transition to chaos in random dynamical systems. In particular, situations are considered where a periodic attractor coexists with a nonattracting chaotic saddle, which can be expected in any periodic window of a nonlinear dynamical system. Under noise, the asymptotic attractor of the system can become chaotic, as characterized by the appearance of a positive Lyapunov exponent. Generic features of the transition include the following: (1) the noisy chaotic attractor is necessarily nonhyperbolic as there are periodic orbits embedded in it with distinct numbers of unstable directions (unstable dimension variability), and this nonhyperbolicity develops as soon as the attractor becomes chaotic; (2) for systems described by differential equations, the unstable dimension variability destroys the neutral direction of the flow in the sense that there is no longer a zero Lyapunov exponent after the noisy attractor becomes chaotic; and (3) the largest Lyapunov exponent becomes positive from zero in a continuous manner, and its scaling with the variation of the noise amplitude is algebraic. Formulas for the scaling exponent are derived in all dimensions. Numerical support using both low- and high-dimensional systems is provided.

DOI: 10.1103/PhysRevE.67.026210 PACS number(s): 05.45.−a, 05.40.−a

I. INTRODUCTION

In this paper, the problem of the transition to chaos in random dynamical systems [1–9] is revisited, and results are presented concerning the topological and scaling aspects of the transition which, to our knowledge, have not been noticed previously. In particular, we consider the setting where, in the absence of noise, the asymptotic attractor of the system is periodic, but nonetheless there is a coexisting chaotic saddle that is nonattracting. This setting is by no means special, because it can occur in every periodic window of a nonlinear system, and it is well known that these windows are dense in the parameter space [10]. When the system is under noise, there can be a transition in the asymptotic attractor from being nonchaotic to chaotic as the noise amplitude is increased through a critical value. For systems described by differential equations, we shall argue that the transition is typically accompanied by a severe topological change in the flow in that the neutral direction of the flow, existing prior to the onset of noisy chaos, is destroyed. Furthermore, we find that the dynamical mechanism for the topological destruction of the neutral direction is unstable dimension variability [11,12], a type of nonhyperbolicity characterized by the existence of periodic orbits along a continuous trajectory with distinct numbers of unstable eigendirections. At a quantitative level, we derive a scaling law for the Lyapunov exponent with the noise variation about the transition. These results are valid for systems in all dimensions, and we believe they are generic and consequently observable in laboratory experiments.

The interplay between chaos and noise has been a topic of continuous interest in nonlinear dynamics and statistical physics [1–9,13]. Transition to noisy chaos is one of the fundamental problems. A brief history of the problem is the following. Crutchfield *et al.* [1] discovered that, in the common route to chaos via the period-doubling bifurcations, noise tends to smooth out the transition and induce chaos in parameter regimes where there is no chaos otherwise. Scaling laws concerning the noisy transition in the period-doubling regime were investigated by Deutsch [2] and by Deutsch and Paladin [4] using the random-matrix approach. The observability and scaling of fractal structures near the transition to chaos in random maps were investigated by Yu *et al.* [6], followed by observation and characterization of such fractal structures formed by floaters on the surface of fluid [14]. Features of transition to chaos in noisy dynamical systems, such as intermittency and the smooth behavior of the Lyapunov exponents, were also found in the transition from strange nonchaotic to strange chaotic attractors in quasiperiodically driven systems [15] and in the bifurcation to chaos with multiple positive Lyapunov exponents in high-dimensional systems [16]. It was also demonstrated [8] that the transition is closely related to the problem of noise-induced synchronization in chaotic systems [13]. Recent works include noise-induced chaos in discrete-time maps and in semiconductor laser systems [7]. Noise-excited chaos is also an important phenomenon in the dynamics of epidemic outbreaks [9].

The focus of this paper is on the transition to chaos in random dynamical systems described by the following general class of stochastic differential equations:

$$\frac{d\mathbf{x}}{dt} = \mathbf{F}(\mathbf{x}, p) + D\xi(t), \tag{1}$$

where $\mathbf{x} \in \Re^N$, $\mathbf{F}$ is the velocity field that can potentially generate chaos, p is a system parameter, and $D\xi(t)$ represents the additive Gaussian white noise of amplitude D[$\xi(t)$ is an N-dimensional vector whose components are independent

Gaussian random variables of zero mean and unit variance]. For a typical trajectory $\mathbf{x}(t)$ on an ergodic, invariant set, the Lyapunov spectrum [17] is

$$\lambda_i = \lim_{T\to\infty} \frac{1}{T} \ln \frac{|\delta \mathbf{x}_i(T)|}{|\delta \mathbf{x}_i(0)|}, \tag{2}$$

where $\{\delta \mathbf{x}_i(t)\}_{i=1}^{N}$ is a set of infinitesimal, orthonormal vectors evolving in the tangent space of the velocity field, as follows:

$$\frac{d\,\delta \mathbf{x}_i(t)}{dt} = \frac{\partial \mathbf{F}(\mathbf{x},p)}{\partial \mathbf{x}} \cdot \delta \mathbf{x}_i(t) \equiv \mathbf{DF}(\mathbf{x},p) \cdot \delta \mathbf{x}_i(t), \tag{3}$$

and $\mathbf{DF}(\mathbf{x},p)$ is the Jacobian matrix evaluated along the trajectory $\mathbf{x}(t)$. Performing the orthonomalization procedure in a proper way, the exponents can be ordered, as follows: $\lambda_1 \geqslant \lambda_2 \cdots \geqslant \lambda_N$, where λ_1 is the largest Lyapunov exponent. Here by *chaos in the random dynamical system* [Eq. (1)], we mean that the largest Lyapunov exponent is positive: $\lambda_1 > 0$. (The resulting attractors, despite the presence of noise in the system, are indeed chaoticlike attractors, as they have the geometric properties similar to those of chaotic attractors in deterministic systems.) In the purely deterministic case ($D=0$), one of the exponents must be zero as the dynamics along the flow is neutral, i.e., it is neither expanding nor contracting. The parameter p is chosen such that the attracting set of the deterministic system $\mathbf{F}(\mathbf{x},p)$ is not chaotic, but nonetheless the system may possess chaotic saddles, either originally existent in the system or induced by noise. The former situation can arise when the dynamical system is in a periodic window. The latter can occur when the system is in a period-doubling parameter region (not in a window) where the stable and unstable manifolds of some unstable periodic orbits have the potential to become tangent and then form a homoclinic or heteroclinic tangle. As such, the presence of small noise can induce the homoclinic or heteroclinic tangencies and create a *stochastic chaotic saddle* [9]. In the absence of noise, the largest Lyapunov exponent of the asymptotic attractor is zero. As the noise is turned on and its amplitude becomes sufficiently large, there is a nonzero probability that a trajectory originally on the attracting set escapes it and wanders near the coexisting chaotic saddle. In this case, the largest Lyapunov exponent becomes positive, signifying chaos for trajectories starting from typical initial conditions. But what are the dynamical characteristics of the transition?

The principal results of this paper are as follows. (1) When the noise amplitude D exceeds a critical value D_c, unstable dimension variability [11,12] can arise in the sense that a typical trajectory moves in phase-space regions containing unstable periodic orbits with distinct numbers of unstable eigendirections. As a result, the transition is smooth in the sense that the largest Lyapunov exponent becomes positive continuously from zero as the noise amplitude is increased. (2) After the transition ($D>D_c$), the topology of the flow is disturbed in a fundamental way: there is no longer a zero Lyapunov exponent, indicating that for noisy chaos, there exists no neutral direction along which infinitesimal distances are conserved, in sharp contrast to deterministic chaotic flows [18] or noisy nonchaotic flows for $D<D_c$. However, for D sufficiently larger than D_c, one Lyapunov exponent becomes increasingly close to zero. The topological destruction of the neutral direction of the flow is, therefore, most severe for $D \gtrsim D_c$. (3) Quantitatively, for $D \gtrsim D_c$, the largest Lyapunov exponent versus the noise amplitude obeys the algebraic scaling law

$$\lambda_1 \sim (D-D_c)^{\alpha}, \tag{4}$$

where α is a scaling exponent that depends on dynamical invariants of the original chaotic saddle such as its Lyapunov exponents and lifetime. We are able to derive formulas for the exponent in *all* dimensions. A surprising finding of our work is that, even in low-dimensional chaotic systems possessing at most one positive Lyapunov exponent, unstable dimension variability can arise due to noise, in contrast to the common belief that this type of nonhyperbolicity usually occurs in high-dimensional systems [12]. A brief account of part of this work appeared recently [19].

The rest of the paper is organized as follows. In Sec. II, we describe the dynamical phenomenon of unstable dimension variability and argue that it must occur for noisy chaotic attractors and it leads to the destruction of the neutral direction of the flow. In Sec. III, we derive the scaling law [Eq. (4)], and give explicit formulas for the scaling exponent in all dimensions. In Sec. IV, we provide numerical support for the scaling formulas with well-studied chaotic flows in representative dimensions. In Sec. V, we introduce a quantity to characterize the degree of the topological destruction of the neutral direction, study the on-off intermittent behavior that typically arises after the transition, and address the validity of the major assumption used in our scaling analysis. In Sec. VI, we present results with a high-dimensional physical system and a nonautonomous system. A discussion is presented in Sec. VII.

II. NOISE-INDUCED UNSTABLE DIMENSION VARIABILITY AND DYNAMICAL CONSEQUENCES

A. Unstable dimension variability

Unstable dimension variability means that, along a typical trajectory, the number of local unstable directions can change. The concept was first conceived by Abraham and Smale [11] who constructed a mathematical model consisting of two unstable fixed points with distinct numbers of local unstable eigendirections. It was later realized that the phenomenon is quite common and can have intricate consequences on the shadowability of numerical trajectories in high-dimensional chaotic systems [12]. To explain unstable dimension variability, we recall here the mathematical definition for hyperbolicity (or nonhyperbolicity) of dynamical systems.

Consider an $(N+1)$-dimensional flow or, equivalently, an N-dimensional map on a Poincaré surface of section: $\mathbf{x}_{n+1} = \mathbf{f}(\mathbf{x}_n)$, where $\mathbf{x} \in \mathcal{R}^N$. Let $\mathbf{\Lambda}$ be an invariant set of $\mathbf{f}$. At any point $\mathbf{x} \in \mathbf{\Lambda}$, the tangent space $\mathbf{T}_\mathbf{x}$ can be split into a direct sum of stable and unstable subspaces: $\mathbf{T}_\mathbf{x} = \mathbf{E}_\mathbf{x}^s \oplus \mathbf{E}_\mathbf{x}^u$. The *stable* and *unstable* manifolds at $\mathbf{x}$ are

$$W^s(\mathbf{x}) = \{\mathbf{y}: \mathbf{f}^n(\mathbf{y}) \to \mathbf{x} \quad \text{as} \quad n \to \infty\}$$

and

$$W^u(\mathbf{x}) = \{\mathbf{y}: \mathbf{f}^{-n}(\mathbf{y}) \to \mathbf{x} \quad \text{as} \quad n \to \infty\},$$

respectively. The stable manifold $W^s(\mathbf{x})$ is tangent to $\mathbf{E}^s_\mathbf{x}$ at $\mathbf{x}$, and the same is true for the unstable manifold $\mathbf{W}^u(\mathbf{x})$ and $\mathbf{E}^u_\mathbf{x}$. The invariant set $\mathbf{\Lambda}$ is hyperbolic if the following properties hold:

(i) The stable and unstable subspaces are distinct, i.e., the angle between $\mathbf{E}^s_\mathbf{x}$ and $\mathbf{E}^u_\mathbf{x}$ is bounded away from zero for every $\mathbf{x} \in \mathbf{\Lambda}$;

(ii) The splitting varies continuously with $\mathbf{x}$ under iterations of $\mathbf{f}$ and is invariant under the Jacobian matrix $\mathbf{Df}(\mathbf{x})$, i.e., $\mathbf{Df}(\mathbf{E}^s_\mathbf{x}) = \mathbf{E}^s_{\mathbf{f}(\mathbf{x})}$ and $\mathbf{Df}(\mathbf{E}^u_\mathbf{x}) = \mathbf{E}^u_{\mathbf{f}(\mathbf{x})}$;

(iii) There exist constants $C > 0$ and $0 < \alpha < 1$ such that $|\mathbf{Df}^n \mathbf{v}| \leqslant C\alpha^n |\mathbf{v}|$ if $\mathbf{v} \in \mathbf{E}^s_\mathbf{x}$ and $|\mathbf{Df}^{-n}\mathbf{u}| \leqslant C\alpha^n |\mathbf{u}|$ if $\mathbf{u} \in \mathbf{E}^u_\mathbf{x}$.

The invariant set $\mathbf{\Lambda}$ is nonhyperbolic if any one of these three conditions is violated. In particular, if condition (i) is violated, there are tangencies between the stable and unstable manifolds. If condition (ii) is violated, there is unstable dimension variability, because the dimension of the local unstable (or stable) subspace can vary with $\mathbf{x}$.

B. Noise-induced unstable dimension variability

We now argue that noise can induce unstable dimension variability. In particular, in the situation where there are two coexisting dynamical invariant sets with distinct unstable dimensions, noise can link the two sets, and thereby induce unstable dimension variability along a continuous trajectory. Such a situation is expected to be fairly common, because it can occur in any periodic window where a periodic attractor and a chaotic saddle coexist. The critical amplitude of the noise for which unstable dimension variability arises is proportional to the phase-space distance between the attractor and the chaotic saddle in the absence of noise, which in turn is proportional to the size of the periodic window in the parameter space. Besides periodic windows, another situation is where there is a periodic attractor and several isolated saddle periodic orbits. The stable and unstable manifolds of these orbits are close to each other, and are about to form homoclinic or heteroclinic intersections. The presence of noise can materialize the intersections, creating a chaotic set, the so-called *stochastic chaotic saddle* [9]. Unstable dimension variability can occur as the noise is increased. The difference from the case of a periodic window is that here, noise induces both the chaotic saddle and unstable dimension variability.

For visual clarity, we illustrate our analysis by focusing on a two-dimensional Poincaré map obtained from a three-dimensional autonomous flow, as shown schematically in Fig. 1, where there are a periodic attractor and a coexisting chaotic saddle. However, the analysis holds in any dimensions. The circular region surrounding the periodic attractor denotes the effective range of the influence of noise of amplitude D, which can be conveniently called the *noisy basin* of the periodic attractor [19]. For clarity, the stable and unstable manifolds of the chaotic saddle are represented by lines, although they too are fattened by noise. For $D < D_c$, there is no overlap between the stable manifold of the chaotic saddle and the noisy basin of the periodic attractor, as shown in Fig. 1(a). In this case, a random initial condition leads to a trajectory confined in the vicinity of the periodic attractor, although there can be transient chaos initially, in the sense that the trajectory may move toward the chaotic saddle along its stable manifold, wander near the saddle for a finite amount of time, and leave it along its unstable manifold. For $D > D_c$, a subset of the stable manifold of the chaotic saddle is located in the noisy basin of the periodic attractor, as in Fig. 1(b). As a result, there is a nonzero probability that a trajectory near the periodic attractor is kicked out of the noisy basin and moves toward the chaotic saddle along its stable manifold. Because the chaotic saddle is nonattracting, the trajectory can stay in its vicinity for only a finite amount of time before leaving along its unstable manifold and then, enter the noisy basin of the periodic attractor again, and so on. For $D \gtrsim D_c$, the probability for the trajectory to leave the noisy basin of the periodic attractor is small. Thus an intermittent behavior can be expected where the trajectory spends long stretches of time near the periodic attractor, with occasional bursts out of it wandering near the chaotic saddle.

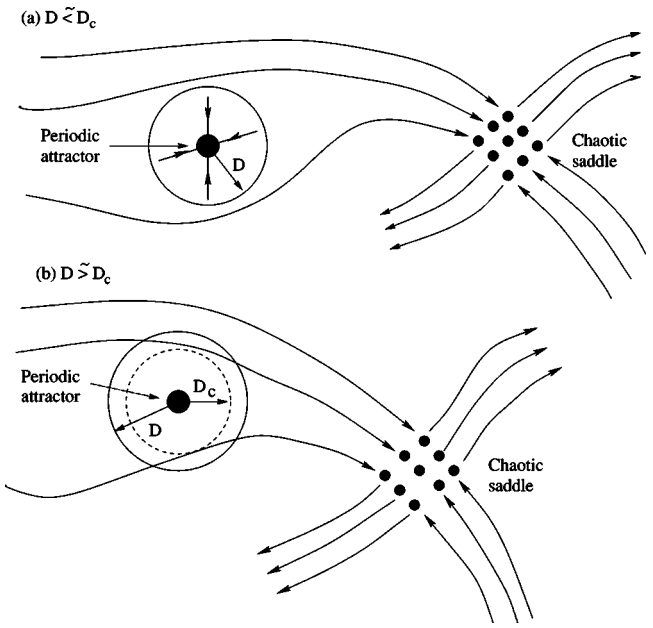

FIG. 1. Schematic illustration of the interplay between the noise and dynamics on a Poincaré surface of section: (a) trajectories are confined near the periodic attractor for $D \lesssim D_c$, and (b) a typical trajectory can move intermittently between the periodic attractor and the chaotic saddle for $D \gtrsim D_c$.

A consequence of the noise-induced intermittent behavior is that there is generally unstable dimension variability associated with a continuous trajectory. Under noise, both the chaotic saddle and the periodic attractor belong to a single, connected dynamical invariant set. As periodic orbits on the chaotic saddle are all unstable and the originally attracting periodic orbit is stable, the noise-induced intermittency

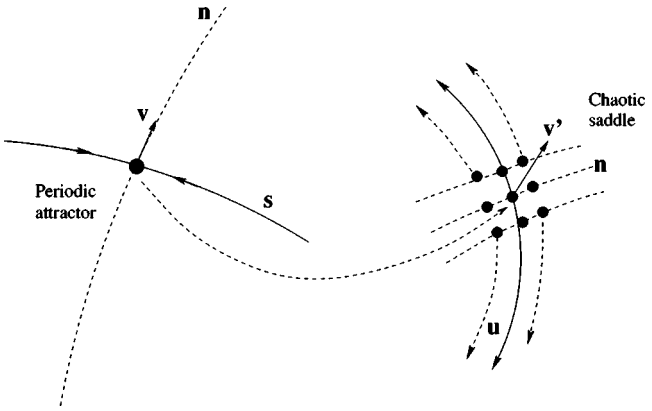

FIG. 2. Schematic illustration of the destruction of the neutral direction of the noisy chaotic flow due to unstable dimension variability. The local planes about the periodic attractor and a point in the chaotic saddle do not coincide in general, and these planes are not in a Poincaré surface of section.

means that a trajectory moves in regions containing periodic orbits with distinct unstable dimensions. A feature that distinguishes this type of unstable dimension variability with that in the literature [12] is that here, the subsets with different unstable dimensions are located in distinct regions of the phase space, whereas in high-dimensional chaotic systems such as the kicked double rotor [12], unstable periodic orbits in these subsets tend to mix with each other in the phase space.

The above argument can be extended to higher-dimensional systems. For instance, one can consider periodic windows in a chaotic region in the parameter space. If the chaotic attractors near the periodic windows have unstable dimension 2 or higher, the chaotic saddle in the window is expected to have the same unstable dimension. Noise can then generate continuous trajectories that move in phase-space regions containing periodic orbits with either two or more unstable directions or none.

C. Destruction of neutral direction of flow

At a fundamental level, after onset of chaos, unstable dimension variability induced by noise will destroy the neutral direction of the flow. For a three-dimensional flow, the original periodic attractor contains no unstable direction, and the chaotic saddle possesses one unstable dimension. The role of noise, when it is sufficiently large ($D>D_c$), is to link these two dynamical invariant sets with distinct unstable dimensions. Now examine the local eigenplanes that contain the neutral direction of the flow associated with the periodic attractor and the chaotic saddle, as shown schematically in Fig. 2. In the local eigenplane about the periodic attractor, there is a stable direction and a neutral direction. Let **v** be the eigenvector in the neutral direction. In the eigenplane of a point in the chaotic saddle, there is an unstable direction and a neutral direction. When a trajectory is driven by noise from the periodic attractor to the chaotic saddle along its stable manifold, the eigenvector **v** maps to **v**′ (see Fig. 2), which can lie anywhere in the local eigenplane of the corresponding point in the chaotic saddle. After a time, the vector will be aligned in the unstable direction, due to the expanding dynamics associated with the chaotic saddle. Distances along the neutral direction of the original periodic attractor can no longer be preserved. In general, a neutral vector associated with a subset can no longer be a neutral one, when the trajectory that ''carries'' the vector moves to another subset with more unstable directions. Thus, we see that unstable dimension variability plays a fundamental role in determining the topology of the flow after onset of noisy chaos.

The disappearance of the neutral direction can also be seen by examining the influence of noise on the spectra of the Lyapunov exponents. Again take a three-dimensional flow as an example. Let $\lambda_3^P \leqslant \lambda_2^P < \lambda_1^P = 0$ and $\lambda_3^S < \lambda_2^S = 0 < \lambda_1^S$ be the Lyapunov spectra of the periodic attractor and of the chaotic saddle, respectively, in the absence of noise. Let $\lambda_3 < \lambda_2 < \lambda_1$ be the Lyapunov spectrum of the noisy attractor. For $D<D_c$, the noisy attractor is only a fattened version of the original periodic attractor. Thus we have $\lambda_i = \lambda_i^P (i = 1,2,3)$ [20]. In particular, there is still a null Lyapunov exponent $\lambda_1 = 0$, despite the presence of noise, indicating that the topology of the flow is preserved. For $D>D_c$, there is an intermittent hopping of the trajectory between regions that contain the original periodic attractor and the chaotic saddle. Let f_P and f_S be the fractions of time that the trajectory spends asymptotically in the corresponding regions. Then we have

$$\begin{aligned} \lambda_1 &\approx f_P \lambda_1^P + f_S \lambda_1^S = f_S \lambda_1^S > 0, \\ \lambda_2 &\approx f_P \lambda_2^P + f_S \lambda_2^S = f_P \lambda_2^P < 0, \\ \lambda_3 &\approx f_P \lambda_3^P + f_S \lambda_3^S < 0. \end{aligned} \tag{5}$$

The remarkable feature is that the Lyapunov spectrum of the noisy attractor now contains no null exponent. Thus, immediately after the noise amplitude exceeds the critical value D_c, the noisy attractor becomes chaotic in the sense that its largest Lyapunov exponent is positive. This chaotic attractor is, however, fundamentally different in its flow topology from any deterministic chaotic attractors in that it no longer contains a neutral direction. We stress that this topological disturbance of the flow exists only for $D>D_c$. For $D<D_c$, the neutral direction of the flow is well preserved, despite the presence of noise.

It should be emphasized that the Lyapunov spectra $\{\lambda_1^P, \lambda_2^P, \lambda_3^P\}$ and $\{\lambda_1^S, \lambda_2^S, \lambda_3^S\}$ in Eq. (5) are defined with respect to the invariant sets, namely, the periodic attractor and chaotic saddle, respectively, in the absence of noise. These sets are located in different regions in the phase space and they are distinct in the sense that, dynamically, they are not mutually connected. That is, in the absence of noise, a point in a set can never move to another set. For $D<D_c$, the two sets can still be regarded as distinct because they are not mutually connected in the sense that, although a point on the chaotic saddle can be moved to the periodic attractor by noise, the converse is not true. For $D>D_c$, the two sets are mutually connected and so are no longer distinct in a strict sense. However, for $D \gtrsim D_c$, a trajectory typically spends long stretches of time near the original periodic attractor with

occasional visits to the chaotic saddle, which occur in a relatively short time. Under this circumstance the sets can be regarded as distinct but only in an approximate sense. That is, Eq. (5) is approximately valid only for $D \gtrsim D_c$.

III. SCALING THEORY

We now derive the general scaling law [Eq. (4)] in all dimensions. Consider an $(N+1)$-dimensional flow in a periodic window. In the absence of noise, the chaotic saddle has K_u positive exponents, one zero exponent, and K_s negative Lyapunov exponents ($K_u+K_s=N$) which can be ordered as follows:

$$\lambda_{K_u}^{S+} \geqslant \lambda_{K_u-1}^{S+} \geqslant \cdots \lambda_1^{S+} > 0 = \lambda^{S0} > -\lambda_1^{S-} \geqslant \cdots \geqslant -\lambda_{K_s-1}^{S-} \geqslant -\lambda_{K_s}^{S-}. \tag{6}$$

The periodic attractor has one zero exponent and N negative exponents, as follows:

$$0 = \lambda^{P0} > -\lambda_1^{P-} > \cdots - \lambda_N^{P-}. \tag{7}$$

For $D<D_c$, an asymptotic trajectory is confined in the neighborhood of the periodic attractor, so the largest Lyapunov exponent of the noisy attractor is simply $\lambda_1 = \lambda^{P0} = 0$. For $D \gtrsim D_c$ (after the transition to chaos), λ_1 is approximately given by

$$\lambda_1 \approx f_P(D)\lambda^{P0} + f_S(D)\lambda_{K_u}^{S+} = f_S(D)\lambda_{K_u}^{S+}. \tag{8}$$

Because of the averaging effect of noise, we expect the dependence on noise of the largest Lyapunov exponent $\lambda_{K_u}^{S+}$ of the original chaotic saddle to be weak. Thus the main dependence of λ_1 on noise comes from $f_S(D)$, the frequency of visit to the chaotic saddle, which is determined by the measure of its stable manifold in the noisy basin of the periodic attractor. To obtain the scaling behavior of $f_S(D)$, it is necessary to examine the natural measure and the dimension formulas for chaotic saddle in general.

A. Natural measures and dimension formulas

1. Natural measure

The dimension spectra of a chaotic saddle and its stable and unstable manifolds are determined by the corresponding natural measures, which can be defined as follows. Imagine a phase-space region S that contains a chaotic saddle. The stable and unstable manifolds of the chaotic saddle are sets of points that asymptote to it under the forward and backward iterations of the map, respectively. If a large number N_0 of random initial conditions are distributed in S, the corresponding trajectories will leave S eventually. They do so by being attracted along the stable manifold, wandering near the chaotic saddle for a finite amount of time, and then exiting along the unstable manifold. Let $N(t)$ be the number of trajectories that still remain in S at time t. Due to the chaotic nature of the saddle, $N(t)$ decreases exponentially in time,

$$N(t) = N_0 e^{-t/\tau}, \tag{9}$$

where τ is the average lifetime of the chaotic transients, and the inverse of which, $\kappa \equiv 1/\tau$, is the escape rate of the saddle [21,22]. Since trajectories escape from the chaotic saddle along the unstable manifold, at large positive time t, the $N(t)$ trajectory points will be in the vicinity of the unstable manifold. Let B be a small box within S that contains part of the unstable manifold. The natural measure associated with the unstable manifold in B can thus be defined as [23,24]

$$\mu_u(B) = \lim_{t\to+\infty} \lim_{N_0\to\infty} \frac{N_u(t,B)}{N(t)}, \tag{10}$$

where $N_u(t,B)$ is the number of the $N(t)$ orbits in B at time t. Similarly, the natural measure of the stable manifold in a box B in S is [23,24]

$$\mu_s(B) = \lim_{t\to+\infty} \lim_{N_0\to\infty} \frac{N_s(t,B)}{N(t)}, \tag{11}$$

where $N_s(t,B)$ is the *number of initial conditions* in B whose trajectories do not leave S before time t.

From definitions (10) and (11), we see that the natural measures associated with the stable and unstable manifolds in B are determined by the numbers of trajectory points in B at time zero and time t, respectively. The natural measure μ of the chaotic saddle can then be defined by considering $N_m(\rho,t,B)$, the number of trajectory points in B at a time ρt in between zero and t,

$$\mu(B) = \lim_{t\to+\infty} \lim_{N_0\to\infty} \frac{N_m(\rho,t,B)}{N(t)}, \tag{12}$$

where $0<\rho<1$, $N_m(0,t,B)=N_s(t,B)$, and $N_m(1,t,B) = N_u(t,B)$. For large N_0 and t, trajectories remaining in S would stay near the chaotic saddle for most of the time between zero and t, except at the beginning when they are attracted toward the saddle along the stable manifold, and at the end when they exit along the unstable manifold. Thus the measure defined in Eq. (12) is independent of ρ, insofar as $0<\rho<1$.

Note that, although $N(t)$ decreases exponentially in time, this decaying factor has been compensated in the definitions of the natural measures [Eqs. (10)–(12)]. These measures are thus invariant under the dynamics, and they are also called the *conditionally invariant measures* [22]. Numerically, the natural measure of the chaotic saddle can be computed by using the sprinkler method [24] or the PIM-triple method [25,26], the latter can generate long trajectories on the chaotic saddle.

To define the fractal dimensions, it is necessary to cover the chaotic saddle with a grid of boxes of size δ. Let μ_i be the natural measure contained in the ith box. The dimension spectrum [27,28] of the chaotic saddle [24,29] is

$$d_q = \lim_{\delta\to 0} \frac{1}{q-1} \frac{\ln \sum_i \mu_i^q}{\ln \delta}. \tag{13}$$

For instance, the information dimension is

$$d_1 = \lim_{\delta \to 0} \frac{\sum_i \mu_i \ln \mu_i}{\ln \delta}. \tag{14}$$

The dimension spectra of the stable and unstable manifolds can be defined similarly based on their natural measures.

2. Dimension formulas

The Kaplan-Yorke conjecture states that the information dimension of a chaotic set is equal to the Lyapunov dimension [30], which can be computed by the Lyapunov exponents of the set. For a chaotic saddle, Hunt *et al.* [29] obtained explicit formulas for the Lyapunov dimensions d_u, d_s, and d of the stable and unstable manifolds of the saddle, and itself, respectively. Consider the N-dimensional map on a Poincaré surface of section. Given the Lyapunov spectrum of the chaotic saddle in Eq. (6), its forward entropy is

$$H^S = \sum_{i=1}^{K_u} \lambda_i^{S+} - \frac{1}{\tau}. \tag{15}$$

Then the dimension of the unstable manifold of the chaotic saddle is

$$d_u = K_u + I + \frac{H^S - (\lambda_1^{S-} + \cdots + \lambda_I^{S-})}{\lambda_{I+1}^{S-}}, \tag{16}$$

where the integer I is determined by

$$\lambda_1^{S-} + \cdots + \lambda_I^{S-} + \lambda_{I+1}^{S-} \geqslant H^S \geqslant \lambda_1^{S-} + \cdots + \lambda_I^{S-}. \tag{17}$$

The dimension of the stable manifold of the chaotic saddle is

$$d_s = K_s + J + \frac{H^S - (\lambda_1^{S+} + \cdots + \lambda_J^{S+})}{\lambda_{J+1}^{S+}}, \tag{18}$$

where J is determined by

$$\lambda_1^{S+} + \cdots + \lambda_J^{S+} + \lambda_{J+1}^{S+} \geqslant H^S \geqslant \lambda_1^{S+} + \cdots + \lambda_J^{S+}. \tag{19}$$

The dimension of the chaotic saddle itself is

$$d = d_u + d_s - N. \tag{20}$$

B. Scaling laws of Lyapunov exponent with noise in low and high dimensions

1. One dimension

For pedagogical purpose, we consider a one-dimensional chaotic map. In this case, the notion of a neutral direction does not exist but, nonetheless, we can show that when the system is in a periodic window, the Lyapunov exponent versus the noise obeys the same scaling law [Eq. (4)]. Let $\lambda^S > 0$ and $\lambda^P < 0$ be the Lyapunov exponents of the chaotic saddle and of the periodic attractor, respectively. We have $K_s = 0$, $K_u = 1$, and $d_u = 1$. The Lyapunov dimensions of the chaotic saddle and its stable manifold are equal:

$$d_s = d = \frac{H}{\lambda^S} = 1 - \frac{1}{\lambda^S \tau}. \tag{21}$$

For an interval of size ϵ, the natural measure of the stable manifold is proportional to ϵ^{d_s}. When the noise is slightly above the critical level ($D \gtrsim D_c$), the length in which the stable manifold penetrates the noisy basin of the periodic attractor is proportional to $(D - D_c)$. We thus have, for the frequency of visit to the chaotic saddle,

$$f_S(D) \sim (D - D_c)^{d_s} \sim (D - D_c)^{1 - (1/\lambda^S \tau)}. \tag{22}$$

Since there is no zero Lyapunov exponent, Eq. (8) becomes

$$\lambda \approx f_P(D) \lambda^P + f_S(D) \lambda^S. \tag{23}$$

For $D \gtrsim D_c$, $f_P(D) \approx 1$, we have

$$\lambda - \lambda^P \approx f_S(D) \lambda^S \sim (D - D_c)^{1 - (1/\lambda^S \tau)}, \tag{24}$$

which is similar to the scaling law (4) with the following scaling exponent:

$$\alpha = 1 - \frac{1}{\lambda^S \tau}. \tag{25}$$

A feature to notice is that in the common situation where the lifetime of the chaotic saddle in a periodic window is large ($\tau \gg 1$), the scaling exponent is expected to be close to unity.

2. Two dimensions

For a two-dimensional (Poincaré) map arising from a three-dimensional flow, consider a circle of size δ. The natural measure of the stable manifold contained within is proportional to

$$\delta^{d_s} = (\delta^2)^{d_s/2},$$

where δ^2 is proportional to the area of the circle and τ is the lifetime of the chaotic saddle of the Poincaré map (τ is thus in the unit of T, the average time that a typical trajectory crosses the Poincaré section). Let $\lambda_1^S > 0 > \lambda_2^S$ be the Lyapunov exponents of the saddle. We have $K_s = 1$, $J = 0$, and $d_s = 2 - (1/\lambda_1^S \tau)$. From Fig. 1(b), we see that for $D \gtrsim D_c$, the area in which the stable manifold of the chaotic saddle penetrates the noisy basin of the periodic attractor is proportional to: $(D^2 - D_c^2)$. We thus have

$$\lambda_1 \sim (D^2 - D_c^2)^{d_s/2} \sim (D - D_c)^{1 - 1/(2\lambda_1^S \tau)}, \tag{26}$$

which is the scaling law [Eq. (4)] with the following scaling exponent:

$$\alpha = 1 - \frac{1}{2\lambda_1^S \tau}. \tag{27}$$

Again, if $\tau \gg 1$, the scaling exponent is close to unity.

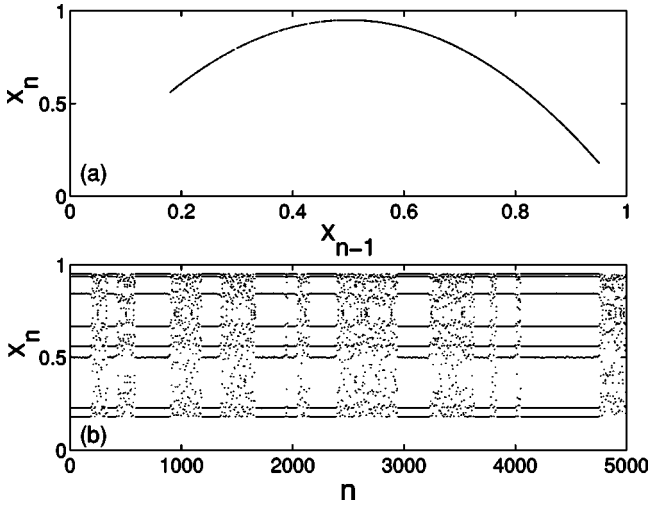

FIG. 3. For the logistic map at parameters $a=3.8008$ and $D=10^{-4.8}\approx 1.6\times 10^{-5}$: (a) noisy chaotic attractor and (b) intermittent time series $\{x_n\}$.

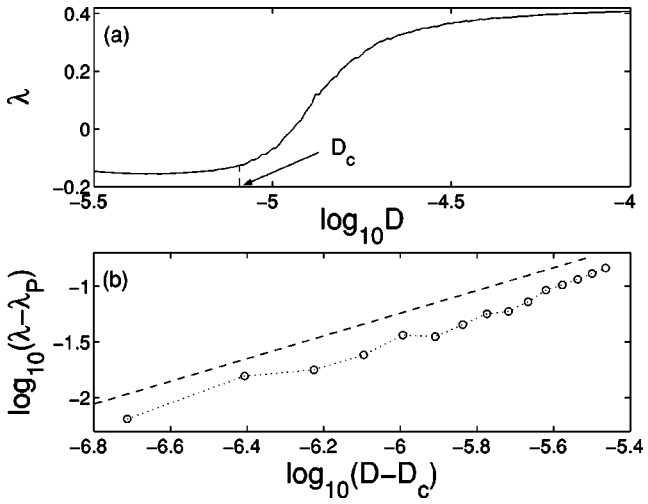

FIG. 4. (a) The increase of the Lyapunov exponent λ vs the noise variation $D-D_c$. The critical noise amplitude is $D_c\approx 10^{-5.1}$. (b) Algebraic scaling between $\lambda-\lambda_P$ and $D-D_c$. The scaling exponent is close to unity (indicated by the dashed line).

3. N dimensions

For an N-dimensional map [or an $(N+1)$-dimensional flow], a similar derivation gives the scaling law [Eq. (4)] with the following scaling exponent:

$$\alpha=\frac{1}{N}\left[K_s+J+\frac{H^S-(\lambda_1^{S+}+\cdots+\lambda_J^{S+})}{\lambda_{J+1}^{S+}}\right]. \tag{28}$$

IV. NUMERICAL RESULTS WITH WELL-STUDIED CHAOTIC SYSTEMS

A. One-dimensional map

In a broad sense, for one-dimensional maps, noise can still induce unstable dimension variability. For instance, in a periodic window, the attractor has only one stable direction while the coexisting chaotic saddle has only an unstable direction. Noise can cause a trajectory to visit both. The issue of interest concerning transition to noisy chaos is then the scaling of the Lyapunov exponent (the neutral direction is not an issue). To demonstrate the validity of the scaling law [Eq. (4)] and the scaling-exponent formula [Eq. (25)], we consider the logistic map [31] $x_{n+1}=ax_n(1-x_n)$, where a is the parameter. There is a periodic window of period 8 for $a=3.8008$. The noisy logistic map is

$$x_{n+1}=ax_n(1-x_n)+D\xi_n, \tag{29}$$

where D is the noise strength and ξ_n is a Gaussian random variable of zero mean and unit variance. Figures 3(a) and 3(b) show, for $D=10^{-4.8}\approx 1.6\times 10^{-5}$, the noisy chaotic attractor in the (x_{n-1},x_n) plane and the time series $\{x_n\}$, respectively. An intermittent behavior can be seen, where the trajectory visits the period-8 attractor and the chaotic saddle coexisting in the window in different times. Figure 4(a) shows the Lyapunov exponent λ versus the noise amplitude, where we observe that $\lambda\approx\lambda_P<0$ for $D<D_c$ and λ starts to increase for $D>D_c$. The critical noise amplitude is estimated to be $D_c\approx 10^{-5.1}$. Figure 4(b) shows $\lambda-\lambda_P$ versus $D-D_c$ on a logarithmic scale, which appears to be algebraic. A least-squares fit gives the following estimate of the scaling exponent: 1.06 ± 0.04. For the logistic map in this period-8 window, the Lyapunov exponent and the lifetime of the chaotic saddle are estimated to be $\lambda^S\approx 0.425$ and $\tau\approx 649$. The theoretical exponent α is thus close to unity, which is consistent with the numerical value.

B. Three-dimensional autonomous flows

1. Rössler system

We consider additive noise to the Rössler oscillator [32]. The system equations are

$$\begin{aligned} dx/dt&=-y-z+D\xi_x(t),\\ dy/dt&=x+0.2y+D\xi_y(t),\\ dz/dt&=0.2+z(x-c)+D\xi_z(t), \end{aligned} \tag{30}$$

where c is the bifurcation parameter, D is the noise amplitute, and $\xi_{x,y,z}$ are independent Gaussian random variables of zero mean and unit variance. Figure 5 shows a bifurcation diagram of the Rössler system in the absence of noise, where the asymptotic values of the dynamical variable y obtained at the Poincaré surface of section $x=0$ are plotted versus the parameter c. We see that periodic windows are quite common. For instance, a period-3 window exists about $c=5.3$. Figure 6(a) shows the projection of the period-3 attractor into the (x,y) plane for $c=5.3$. To study the effect of noise, we fix c at this value and examine the dynamics as noise amplitude is increased from zero. We use the standard second-order Milshtein method [33] to integrate stochastic differential equations (30). We find that chaos arises for $D>D_c\approx 10^{-2.26}\approx 5.5\times 10^{-3}$. For $D\gtrsim D_c$, the asymptotic trajectory of the system is confined in the neighborhood of the original period-3 attractor most of the time, as shown in Fig.

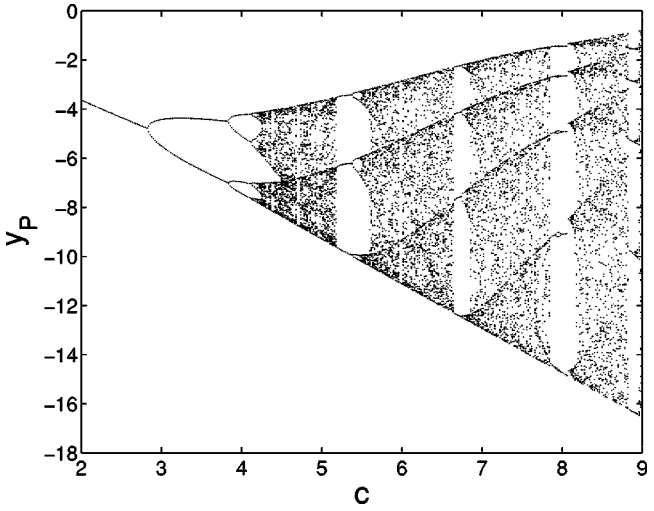

FIG. 5. Bifurcation diagram of the noiseless Rössler system.

6(b) for $D=0.01$. For a larger value of D, the trajectory appears to spend relatively more time in the region where the original chaotic saddle resides, as shown in Fig. 6(c). Figure 7(a) shows the first two Lyapunov exponents of the asymptotic attractor versus the noise amplitude D. We see that for $D<D_c$, the largest Lyapunov exponent is zero, indicating that the noisy flow is not chaotic. The presence of the null Lyapunov exponent means that, in spite of noise, there is a neutral direction associated with the flow. For $D>D_c$, the largest Lyapunov exponent becomes positive, so the noisy flow is chaotic. The remarkable phenomenon is that there is no longer a null Lyapunov exponent, indicating the disappearance of the neutral direction for noisy chaotic flow. Thus the topology of the noisy flow is disturbed fundamentally after the onset of chaos by unstable dimension variability, as we have argued. Figure 7(b) shows, for $D \gtrsim D_c$, the scaling of the largest Lyapunov exponent of the noisy chaotic attractor with $D-D_c$, which is apparently algebraic. A least-squares fit between $\log_{10}\lambda_1$ and $\log_{10}(D-D_c)$ gives the slope of 0.94 ± 0.03.

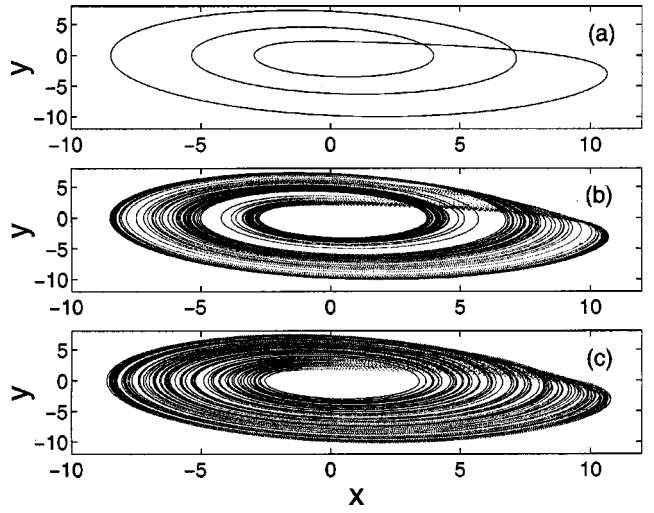

FIG. 6. Asymptotic trajectory of the Rössler system for (a) $D=0$, (b) $D=0.01$, and (c) $D=0.02$.

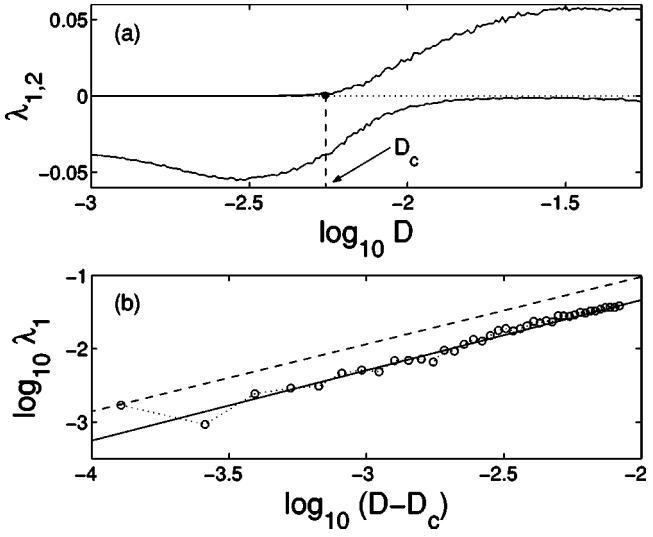

FIG. 7. For the Rössler system, (a) the first two Lyapunov exponents vs D about the transition, and (b) algebraic scaling of the largest Lyapunov exponent with $D-D_c$. From (a), we see that there is no longer a neutral direction of the flow for $D>D_c$. The dashed line in (b) indicates the theoretical slope α.

The theoretically predicted algebraic scaling exponent α in Eq. (27) involves two quantities τ and λ_1^S, the average lifetime and the largest Lyapunov exponent of the original chaotic saddle, respectively. To compute τ, we set $D=0$, use a large number of transient chaotic trajectories, and count the number $N(t)$ of trajectories that have not fallen in the neighborhood of the periodic attractor at time t. The inverse of the rate of the exponential decay in $N(t)$ gives τ. The decay law can be conveniently computed on a Poincaré surface of section. Say one obtains $N(n)\sim e^{-\kappa n}$, where n is the discrete time and κ is the decay rate. The actual lifetime is thus given by $\tau=T/\kappa$, where T is the average return time of the flow to the Poincaré section. To estimate λ_1^S, there are different ways. (1) One can compute the finite-time Lyapunov exponents for many transient chaotic trajectories and construct a histogram of the exponents. In particular, one can distribute a large number of initial conditions in the phase space and choose those whose trajectories behave chaotically for a relatively long time. These constitute approximately an ensemble of initial conditions that can be regarded as being distributed according to the natural measure of the chaotic saddle. For each such initial condition, the corresponding Lyapunov spectrum can be computed in finite time n, yielding the probability distributions for the distinct exponents of the chaotic saddle. For a chaotic set, the distributions are approximately Gaussian with width that decreases in time according to $1/\sqrt{n}$ [34]. The centers of the distributions are the asymptotic values of the corresponding exponents, if an infinite number of initial conditions is used. The center of the distribution of the largest exponent is thus a good approximation of λ_1^S for a finite number of initial conditions. (2) For a periodic window that is relatively small in size in the parameter axis, the Lyapunov exponents of the chaotic saddle in the window are approximately the same as the exponents for a chaotic attractor at a parameter value slightly before or after the window.

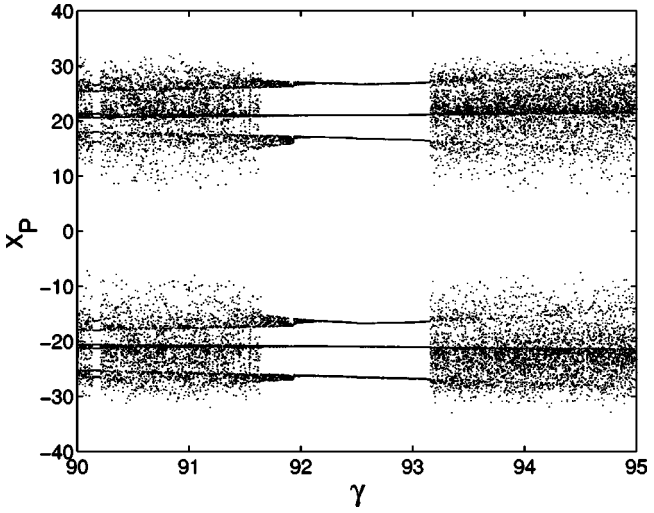

FIG. 8. Bifurcation diagram of the noiseless Lorenz system. The Poincaré surface of section used to compute the diagram is $z=\gamma-1$.

We use the second approach to obtain an estimated value for λ_1^S. For the Rössler system, we obtain $\tau\approx 24.1$ and $\lambda_1^S \approx 0.35$, which gives $\alpha\approx 0.94$. We see that there is an excellent agreement between the theoretical scaling law [Eq. (4)] and numerics.

2. Lorenz system

We next consider the noisy Lorenz system [35],

$$dx/dt = 10(y-x) + D\xi_x(t),$$

$$dy/dt = \gamma x - y - xz + D\xi_y(t), \tag{31}$$

$$dz/dt = -(8/3)z + xy + D\xi_z(t),$$

where γ is the bifurcation parameter, and $\xi_{x,y,z}$ are independent Gaussian random variables of zero mean and unit variance. Figure 8 shows a bifurcation diagram containing a periodic window, where the asymptotic values of the dynamical variable $x(t)$ at the Poincaré surface of section $z=\gamma-1$ is plotted against γ. In the parameter range there is a period-6 window. We fix $\gamma=92.8$. The period-6 attractor in the absence of noise is shown in Fig. 9(a). As noise is turned on, the structure of the attractor appears to become progressively more complicated, as shown in Figs. 9(b) and 9(c) for $D=0.06$ and $D=0.2$, respectively. The behavior of the Lyapunov exponents versus the noise amplitude is shown in Fig. 10(a), which is similar to that of the Rössler system. We see that, for small noise, the largest Lyapunov exponent is zero, indicating that the trajectory is still confined in the vicinity of the period-6 attractor. Transition to chaos occurs at $D=D_c\approx 10^{-1.46}\approx 0.025$. For $D>D_c$, the largest Lyapunov exponent becomes positive, and the neutral direction of the flow is destroyed. The algebraic scaling of the largest Lyapunov exponent versus $(D-D_c)$ is shown in Fig. 10(b), where the numerical scaling exponent is estimated to be 0.97 ± 0.03. The theoretical exponent is estimated to be about 0.99 ($\lambda_1^S\approx 0.59$ and $\tau\approx 75.0$). There is again a good agreement between numerics and theory.

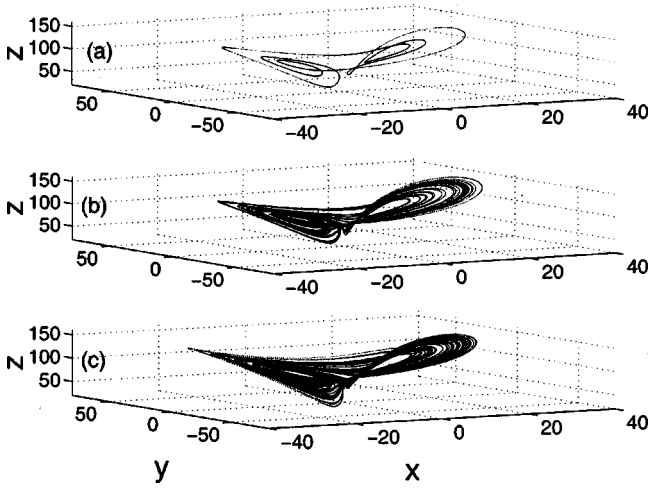

FIG. 9. For the Lorenz system in a period-6 window, the attractor for (a) $D=0$, (b) $D=0.06$, and (c) $D=0.2$.

C. Coupled Rössler system

As a high-dimensional example, we consider the following system of two coupled Rössler chaotic oscillators [32] under noise:

$$dx_{1,2}/dt = -y_{1,2} - z_{1,2} + K(x_{2,1} - x_{1,2}) + D\xi_{1,2}^1(t),$$

$$dy_{1,2}/dt = x_{1,2} + 0.2y_{1,2} + D\xi_{1,2}^2(t), \tag{32}$$

$$dz_{1,2}/dt = 0.2 + z_{1,2}(x_{1,2} - 5.3) + D\xi_{1,2}^3(t),$$

where K is the coupling strength. For small coupling, the chaotic set of the system can have two positive Lyapunov

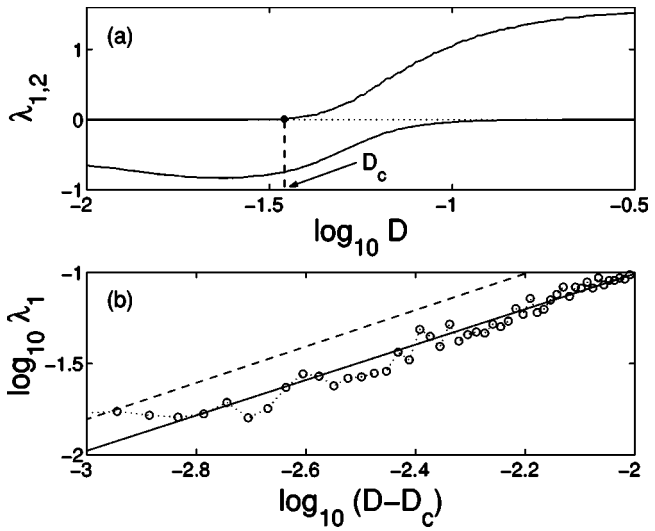

FIG. 10. For the noisy Lorenz system in a period-6 window: (a) the first two Lyapunov exponents near the transition to chaos; (b) algebraic scaling of the largest Lyapunov exponent after the onset of chaos. The dashed line indicates the theoretical slope.

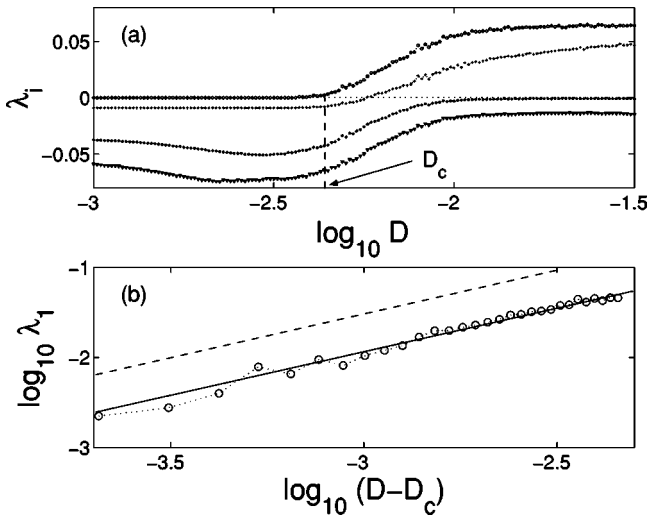

FIG. 11. For the noisy coupled Rössler system [Eq. (32)] in a period-3 window, (a) the first four Lyapunov exponents near the transition to chaos, and (b) algebraic scaling of the largest Lyapunov exponent after the onset of chaos. The dashed line indicates the theoretical slope.

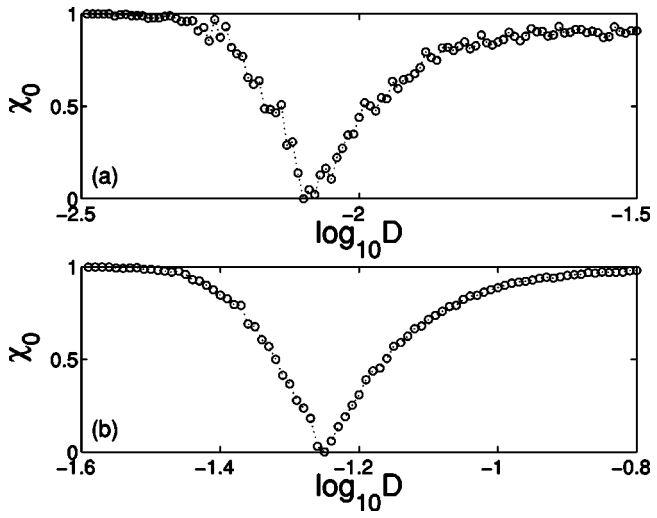

FIG. 12. The topological rigidity χ_0 vs the noise amplitude for (a) the Rössler and (b) the Lorenz systems.

exponents. A period-3 window exists for $K=0.01$ in which there is a periodic attractor and a chaotic saddle with two positive exponents. Figure 11(a) shows the first four Lyapunov exponents of the attractor versus the noise amplitude D. Transition to chaos occurs at $D=D_c\approx 10^{-2.36}\approx 0.0044$, where for $D>D_c$, there is a positive Lyapunov exponent and the noisy chaotic flow has no neutral direction. Figure 11(b) shows the algebraic scaling of λ_1 with $D-D_c$, where the numerical scaling exponent is approximately 1.02 ± 0.02. To estimate the theoretical exponent α, we note that for Eq. (32), $N=5$, $K_s=3$, and $J=1$. Computations give $\lambda_1^+\approx 0.34$, $\lambda_2^+\approx 0.29$, and $\tau\approx 113.2$, and $H=\lambda_1^+ + \lambda_2^+ - 1/\tau\approx 0.62$. Equation (28) thus yields the value of α

$$\alpha=\frac{1}{5}\left(3+1+\frac{\lambda_2^+-\tau^{-1}}{\lambda_2^+}\right)\approx 0.99,$$

which agrees with the numerical result.

V. TOPOLOGICAL RIGIDITY, INTERMITTENCY, AND VALIDITY OF SCALING ASSUMPTION

A. Tolological rigidity

From the numerical examples with continuous-time flows in Sec. IV, we see that the topology of the noisy chaotic flow after the transition is fundamentally different from that of the noisy but nonchaotic flow before the transition. To characterize this change in the flow topology, we introduce the quantity

$$\Delta_0=\min|\lambda_i| \quad \text{for} \quad i=1,\ldots,N, \tag{33}$$

which is the minimum of the absolute value of the Lyapunov exponent closest to zero. Thus, as can be seen from Figs. 7(a), 10(a), and 11(a), Δ_0 first increases from zero as D is strengthened from D_c, reaches maximum at some $D_m \geqslant D_c$, and then decreases asymptotically to zero as D is increased further, mimicking a resonance-like behavior. The quantity Δ_0 is thus a measure of the degree of the topological disturbance to the deterministic flow by noise. Let Δ_0^m be the value of Δ_0 at D_m, the following quantity can be defined:

$$\chi_0=1-\frac{\Delta_0}{\Delta_0^m}, \tag{34}$$

where if $\chi_0=1$, the topology of the flow is preserved in the sense that there is a neutral direction and $\chi_0=0$ indicates a severe destruction of such a topology. Equivalently, χ_0 also measures the degree of noise-induced unstable dimension variability, which is most severe if $\chi_0=0$. We call χ_0 the *topological rigidity* of the flow [36]. Figures 12(a) and 12(b) show, for the Rössler and Lorenz systems studied in Sec. IV B, respectively, χ_0 versus the noise amplitude D. The resonantlike behavior in χ_0 is apparent. Note that this topological aspect of the influence of noise is meaningful only for continuous-time flows.

B. Intermittency

The mechanism of the transition to chaos as the noise amplitude is increased, which is supported by numerical examples in Sec. IV, indicates that a typical trajectory is confined in the neighborhood of the original periodic attractor for $D<D_c$. For $D\gtrsim D_c$, there is a small probability that the trajectory can escape the original attractor and visit the original chaotic saddle. As the saddle is nonattracting, the trajectory will be attracted to the attractor, and so on. An intermittent behavior is then expected for $D\gtrsim D_c$, in which a trajectory spends most of the time in the vicinity of the original periodic attractor with occasional bursts out of the attractor. If we regard motions near the attractor as an ''off'' state and the bursts as an ''on'' state, there is then on-off intermit-

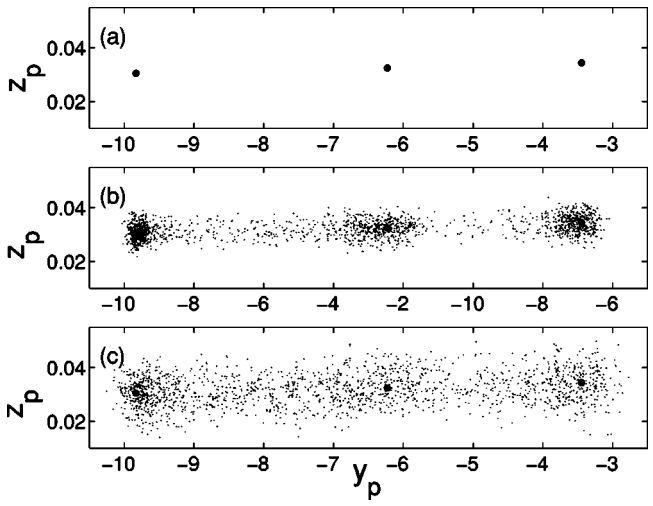

FIG. 13. For the noisy Rössler system in the period-3 window, the behaviors of a trajectory on the Poincaré plane (y_p, z_p) defined by $x=0$ for (a) $D=0$, (b) $D=0.01$, and (c) $D=0.02$.

tency [6,37–39]. But what are the characteristics of the on-off intermittency associated with a noise-induced transition to chaos?

For continuous-time flows, numerically, the intermittent behavior can be conveniently visualized on a Poincaré surface of section. Figures 13(a)–13(c) show, for the Rössler oscillator in the period-3 window studied in Sec. IV B 1, trajectories on the Poincaré plane (y_p, z_p) defined by $x=0$ for $D=0$, $D=0.01$, and $D=0.02$, respectively. For $D \gtrsim D_c$ [panel (b)], the trajectory tends to concentrate on the original period-3 attractor [panel (a)] with occasional motion outside the attractor wandering in a chaotic manner. For the three-times iterated map on the Poincaré section, the period-3 attractor becomes a fixed point. Let $(\Delta y_p, \Delta z_p)$ be the deviation of a trajectory from the fixed point. We expect the time traces of $\Delta y_p(n)$ and $\Delta z_p(n)$ to exhibit an on-off intermittency for $D \gtrsim D_c$, as shown in Figs. 14(a) and 14(b) for $D=0.01$ and 0.02, respectively. The intermittent behavior can

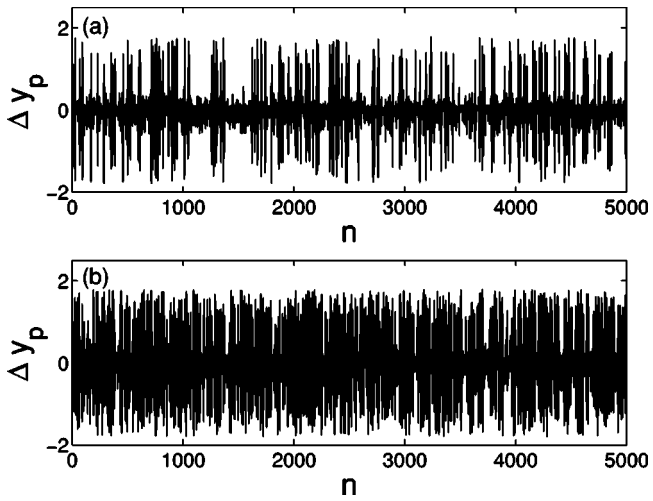

FIG. 14. For the noisy Rössler system in the period-3 window, on-off intermittency in $\Delta y_p(n)$ for (a) $D=0.01$ and (b) $D=0.02$.

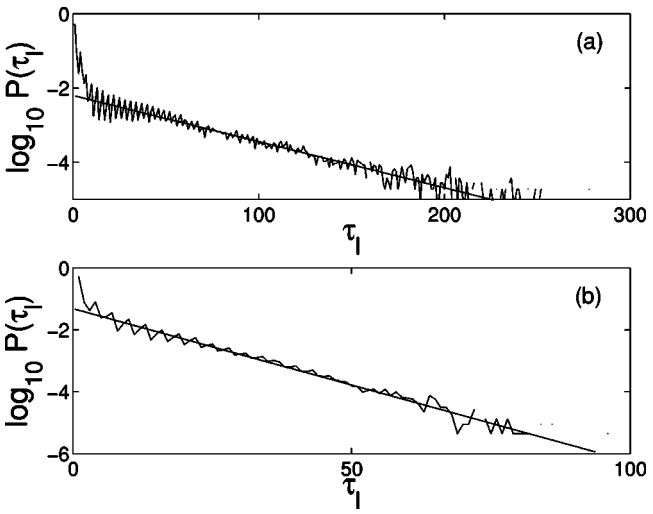

FIG. 15. For the noisy Rössler system in the period-3 window, laminar-phase distributions of the on-off intermittency for (a) $D=0.01$ and (b) $D=0.02$. The distributions are apparently exponential.

be characterized by the laminar-phase distribution, that is, the probability distribution of the time that the trajectory spends in the ''off'' state. Figures 15(a) and 15(b) show, on a semilogarithmic scale, the laminar-phase distributions $P(\tau_l)$ for $D=0.01$ and $D=0.02$, respectively, where τ_l denotes the time interval during which the trajectory is in the ''off'' state. For Figs. 15(a) and 15(b), τ_l is obtained by setting an arbitrary numerical threshold $\Delta\overline{y_p}$ in Figs. 14(a) and 14(b). The apparently linear behavior in the plot of $\log P(\tau_l)$ versus τ_l indicates that the laminar-phase distribution is *exponential*.

Similar behaviors also occur for the Lorenz system. We focus on the period-6 window studied in Sec. IV B 2. Figures 16(a)–16(c) show typical trajectories on the Poincaré plane (x_p, y_p) defined by $z=\gamma-1$ for $D=0$, $D=0.06$, and $D=0.2$, respectively. Because of the robust one-dimensional

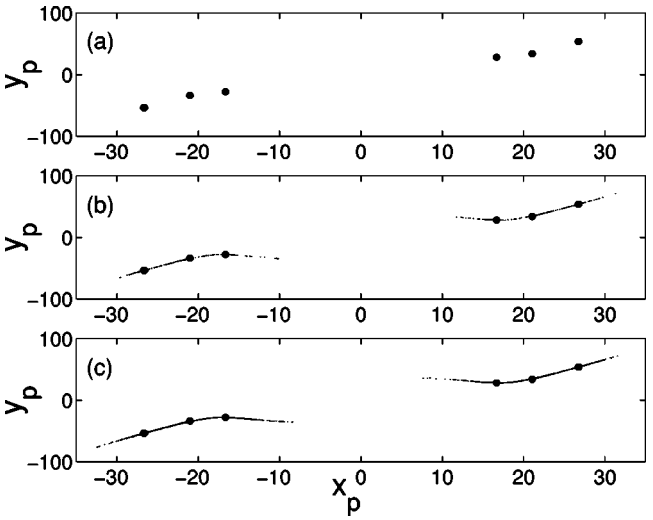

FIG. 16. For the noisy Lorenz system in the period-6 window, the behaviors of a trajecotry on the Poincaré plane (x_p, y_p) defined by $z=\gamma-1$ for (a) $D=0$, (b) $D=0.06$, and (c) $D=0.2$.

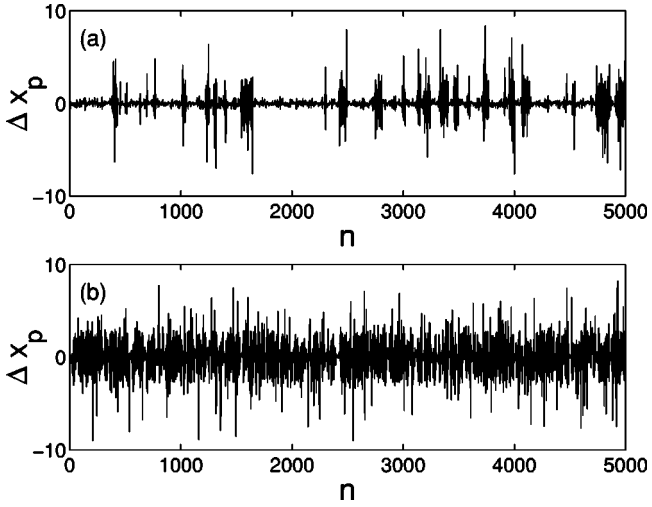

FIG. 17. For the noisy Lorenz system in the period-6 window, on-off intermittency in $\Delta x_p(n)$ for (a) $D=0.06$ and (b) $D=0.2$.

structure of the chaotic Lorenz system, under noise the trajectory tends to move approximately along a one-dimensional curve. Figures 17(a) and 17(b) show the on-off intermittent behavior in the variable $\Delta x_p(n)$ for $D=0.06$ and 0.2, respectively, which is the x component of the deviation of the trajectory from the original period-6 attractor on a six-times iterated map on the Poincaré plane. The laminar-phase distributions of the on-off intermittency are apparently exponential, as shown in Figs. 18(a) and 18(b) for $D=0.06$ and $D=0.2$, respectively.

In most previous works on on-off intermittency [37,38], the laminar-phase distributions appear to be algebraic, at least for small times. In fact, as pointed out in Ref. [38], in a typical system setting of on-off intermittency where the phase space contains an invariant subspace, the laminar-phase distribution is strictly algebraic with the universal scaling exponent of $-3/2$ *at the onset* of on-off intermittency.

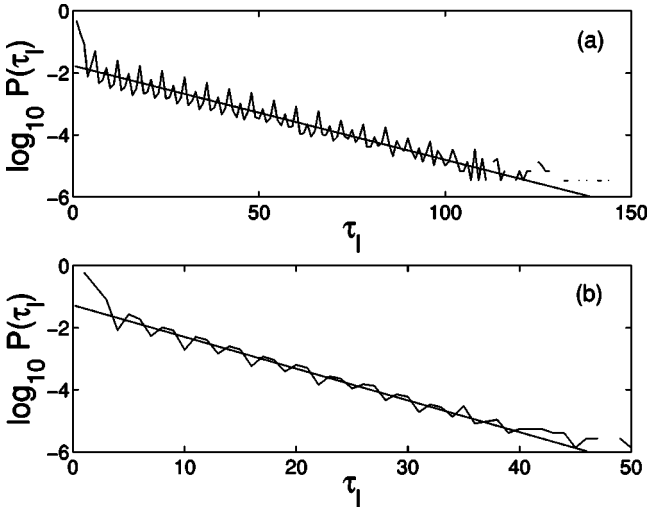

FIG. 18. For the noisy Lorenz system in the period-6 window, laminar-phase distributions of the on-off intermittency for (a) $D=0.06$ and (b) $D=0.2$. The distributions are exponential.

Away from the onset, the distribution is algebraic for small τ_l but has an exponential tail for large τ_l,

$$P(\tau_l)\sim \tau_l^{-3/2} e^{-\beta\tau_l}, \tag{35}$$

where $\beta>0$ is a constant. A more recent study indicates that the exponential behavior tends to dominate if there is a symmetry-breaking [39]. The robust exponential scaling behavior observed for almost all times in Figs. 15 and 18 thus suggests that there is a symmetry breaking in the underlying system, generating on-off intermittency associated with noise-induced transition to chaos.

The exponential distribution of the laminar phases associated with the transition to chaos in discrete-time random maps was observed and analyzed in Ref. [6]. Here we wish to point out that the behavior can also be understood by considering an on-off intermittent process with symmetry breaking. In particular, we consider a one-dimensional variable $X(n)$ characterizing the deviation between the trajectory and original periodic attractor on a Poincaré surface of section. (The null Lyapunov exponent is thus irrelevant for our consideration here.) The largest nontrivial Lyapunov exponent λ is negative for $D<D_c$ and slightly positive for $D \gtrsim D_c$. In finite times, there are fluctuations in the exponent. Approximately, the dynamics of $X(n)$ obeys

$$X(n+1)=\exp[\lambda_1+\eta_1\xi_1(n)]X(n)+bf(X_n)+\eta_2\xi_2(n), \tag{36}$$

where $\eta_1\xi_1(n)$ is a zero-mean chaotic process that simulates the fluctuations of the finite-time Lyapunov exponent, $bf(X_n)$ models symmetry-breaking, and $\eta_2\xi_2(n)$ represents the noise term. Introducing a new variable $Y=-\ln X$, Eq. (36) becomes, approximately, a random walk,

$$Y_{n+1}=Y_n+\nu_n, \tag{37}$$

where ν_n is determined by the symmetry-breaking term, the noise, and the fluctuations of the finite-time Lyapunov exponent. In general, we expect $\langle \nu_n\rangle \neq 0$ and in fact, it can be large because of symmetry breaking [39]. The average drift of the random walk is given by $\bar{\nu}=\int \nu F(\nu)d\nu \neq 0$, where $F(\nu)$ is the probability distribution of ν. To solve the random walk, one can write down the associated Fokker-Planck equation,

$$\frac{\partial P}{\partial t}+\bar{\nu}\frac{\partial P}{\partial Y}=D\frac{\partial^2 P}{\partial Y^2}, \tag{38}$$

where $P(Y,t)$ is the probability distribution of finding the walker at location Y at time t and $D=\int(\nu-\bar{\nu})^2F(\nu)d\nu$ is the diffusion coefficient. A detailed solution to Eq. (38) for on-off intermittency with symmetry breaking can be found in Ref. [39], which predicted that the distribution of the laminar phase is exponential, insofar as a parameter characterizing the symmetry breaking is not zero, no matter how small. Biased random walks thus represent a plausible mechanism

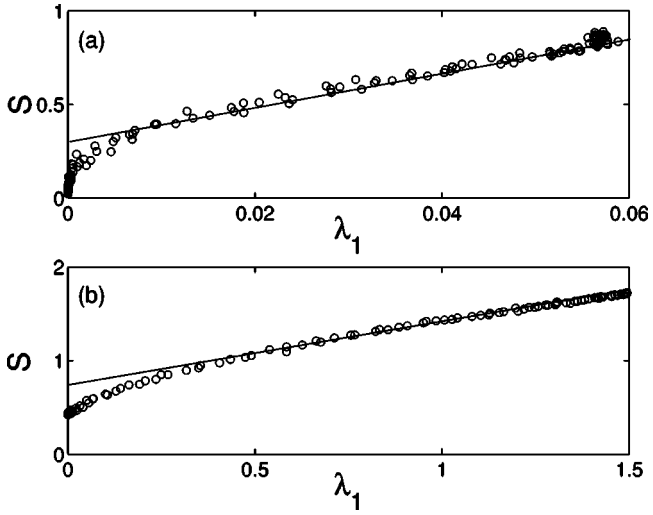

FIG. 19. After transition to chaos, linear dependence of the average bursting amplitude of on-off intermittency on the largest Lyapunov exponent for (a) the Rössler system in the period-3 window and (b) the Lorenz system in the period-6 window studied in Sec. IV.

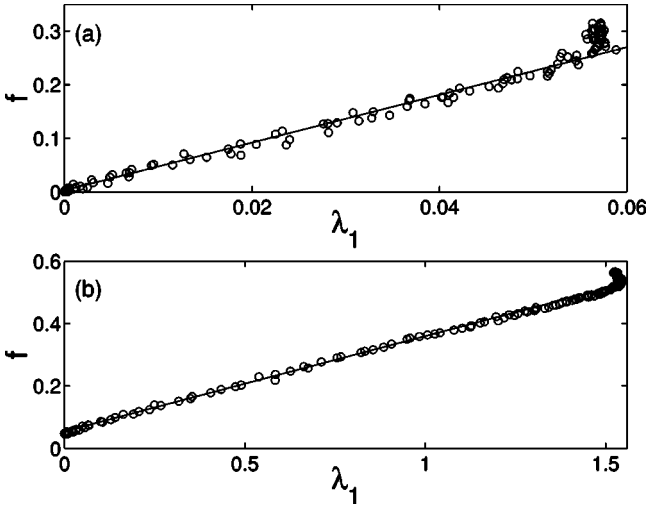

FIG. 20. After transition to chaos, linear dependence of the largest Lyapunov exponent λ_1 on *f*, the frequency of visit to the original chaotic saddle for (a) the Rössler system in the period-3 window and (b) the Lorenz system in the period-6 window studied in Sec. IV.

to account for the on-off intermittent behavior associated with noise-induced chaos near its onset.

Another aspect of the on-off intermittency concerns the average amplitude of the bursts. Yu *et al.* [6] predicted that, for a fixed noise amplitude, the average size of the bursts scales linearly with a system parameter. We note that the purpose of Ref. [6] is to understand the fractal distribution of floaters on the surface of a fluid based on transition to chaos in random maps. The natural setting is thus to fix the noise amplitude and to investigate how a chaotic attractor arises in the underlying random map as a system parameter is varied. In such a setting, the largest Lyapunov exponent scales linearly with the variation of system parameter from the critical value. Our setting is different in that we focus on the transition to chaos as the noise amplitude is increased, for fixed system parameters. Assuming the system is in a periodic window of period *p*, to define the average bursting amplitude, we focus on the *p*-times-iterated map on a Poincaré surface of section and examine the deviation *S* of the trajectory $\mathbf{x}_p$ from the fixed point $\mathbf{x}_p^f$ of the map (which corresponds to the original period-*p* attractor),

$$S \equiv \sqrt{\langle |\mathbf{x}_p - \mathbf{x}_p^f|^2 \rangle}, \tag{39}$$

where $\langle \cdot \rangle$ can be either the ensemble or time averages. Because of the algebraic dependence of λ_1 on the noise difference $(D-D_c)$, we expect the dependence of *S* on $(D-D_c)$ not to be linear, but the dependence of *S* on λ_1 should be approximately linear, as shown in Fig. 19, where panels (a) and (b) are for the Rössler system in the period-3 window and for the Lorenz systems in the period-6 window studied in Sec. IV, respectively.

C. Validity of scaling assumption

The base of our scaling analysis is Eq. (8), which states that for $D \gtrsim D_c$, the largest Lyapunov exponent λ_1 is proportional to the frequency of visit to the original chaotic saddle. How good is this assumption? To provide a justification, we compute the frequency *f* for $D \gtrsim D_c$ and plot it against λ_1, as shown in Figs. 20(a) and 20(b) for the Rössler and Lorenz systems considered in Sec. IV. The linear dependence of λ_1 on *f* appears to be robust.

VI. MORE EXAMPLES

A. A high-dimensional physical example

In this physical example, we show that the requirement of the coexistence of a periodic attractor and a chaotic saddle can be relaxed to the coexistence of a chaotic attractor and a nonattracting chaotic saddle. Here noise can cause the chaotic attractor to develop an additional positive Lyapunov exponent and, remarkably, this exponent scales algebraically with the noise variation as predicted.

As shown in Fig. 21, our system consists of a pendulum of length L_p, mass M_p, and viscous dissipation with coefficient C_p attached to the lower end *B* of a linear viscoelastic rod of length L_r, cross section A_r, mass density ρ_r, elasticity modulus E_r, and coefficient of internal viscous dissipation C_r [41]. The upper end *A* of the rod is subject to a periodic motion $x_A(t)$, resulting in a body force throughout the rod. We restrict the rod to undergo motions along its longitudinal axis *x* and the pendulum to planar motions. Let $u(x,t)$ and $\theta(t)$ denote, respectively, the displacement field of the rod with respect to A and the angular displacement of the pendulum mass.

Let $\xi = x/L_r, \tau = \omega_p t$ (derivative with respect to τ is denoted by a "dot"), where $\omega_p^2 = g/L_p$ is the natural frequency of the uncoupled pendulum, denote normalized spatial and temporal variables, respectively. Let $U = u/L_r$ be the dimensionless displacement field for the rod. The dynamics of the rod-pendulum configuration are described by

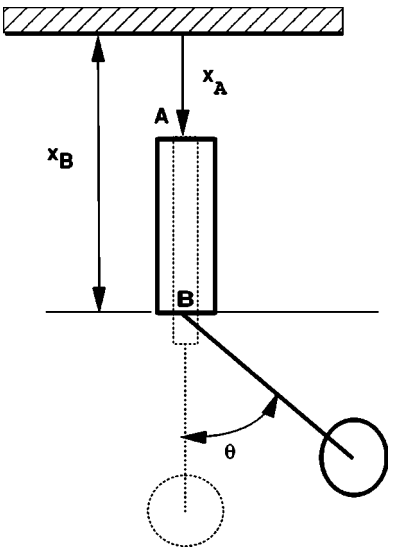

FIG. 21. The geometry of the rod-pendulum system. The dotted configuration is the stable equilibrium.

$$\ddot{\theta} = -[1 - \ddot{V}_B(\tau) + \ddot{X}_A(\tau)]\sin(\theta) - 2\zeta_p\dot{\theta}, \tag{40}$$

$$\frac{\mu^2\pi^2}{4}\frac{\partial^2 V(\xi,\tau)}{\partial\tau^2} = \frac{\partial^2 V(\xi,\tau)}{\partial\xi^2} + 2\zeta_r\mu\frac{\partial^3 V(\xi,\tau)}{\partial\tau\partial\xi^2} - \frac{\mu^2\pi^2}{4}\ddot{X}_A(\tau), \tag{41}$$

$$V(\xi=0,\tau) = 0,$$

$$\frac{\partial V}{\partial\xi}(\xi=1,\tau) = -\frac{\mu^2\beta\pi^2}{4}[1 - T\cos(\theta)], \tag{42}$$

where

$$V(\xi,\tau) = U(\xi,\tau) - \hat{U}(\xi), \tag{43}$$

$$\hat{U}(\xi) = \frac{\mu^2\pi^2}{8}[2(1+\beta)\xi - \xi^2], \tag{44}$$

$$T \equiv \frac{T_p}{M_p L_p \omega_p^2} = \dot{\theta}^2 + [1 - \ddot{X}_B(\tau)]\cos(\theta), \tag{45}$$

$X_A(\tau) = x_A(\tau)/L_p$, and $X_B(\tau) = x_B(\tau)/L_p$. The variable $V(\xi,\tau)$ denotes the normalized displacement field with respect to the normalized static displacement field $\hat{U}(\xi)$ (44), and $V_B(\tau) \equiv V(\xi=1,\tau)$. Equation (42) gives the boundary conditions for the coupled rod [Eq. (41)]. Note that the frequency of the uncoupled pendulum [Eq. (40)] and those of the rod [Eq. (41)] are respectively normalized to unity and to $\mu_m = \omega_1/\omega_m = 1/(2m-1), m = 1,2,\ldots,\infty$, where $\omega_m^2 = \pi^2(2m-1)^2 E_r/L_r^2\rho_r$ (the original natural frequencies of the uncoupled rod). The dissipation factors for the pendulum and the rod are given respectively by $\zeta_p = C_p/2\omega_p L_p M_p$ and $\zeta_r = C_r/8\omega_1\pi^2 L_r^2\rho_r$. Equation (45) gives the normalized tension T along the pendulum arm.

In the above model, the physical parameters that control the coupling between the pendulum and the rod are the frequency ratio $\mu = \omega_p/\omega_1$ and the mass ratio $\beta = M_p/A_r\rho_r L_r$. For a fixed β, the limit of the coupled system [Eq. (40)] as $\mu \to 0$ describes the motions of the parametrically forced uncoupled pendulum. That is, the coupling is one way due to the driving $X_A(t)$, which we assume to be periodic with period $2\pi/\omega$. However, in reality, the driving is always perturbed by a small component of the displacement forces. So we assume a very small perturbation in the frequency of the driving below.

A modal expansion of the $V(\xi,\tau)$ reduces the coupled system to the following set of coupled oscillators, which we truncate for our simulations. We include a separate periodic driving as a limit-cycle solution which contains a variation in the driving frequency ω due to the velocity of the pendulum,

$$\dot{y}_1 = y_2,$$

$$\dot{y}_2 = \frac{1}{\delta}\Big[-2\zeta_1\delta y_2 + \frac{1}{2}\beta^2 y_2^2\sin(2y_1) - (\sin y_1)y_3 + 1 + \beta + 2\zeta y_4 + \delta\alpha\Big(1 + \frac{1}{\beta}\Big)y_6\Big],$$

$$\dot{y}_3 = \frac{y_4}{\mu},$$

$$\dot{y}_4 = \frac{1}{\delta\mu}[-y_3 - 2\zeta y_4 + \beta y_2^2\cos y_1 + \delta(1-\alpha y_6) - (1+\beta)],$$

$$\dot{y}_5 = y_5 + \omega(0.1 + \sigma y_2)y_6 - y_5(y_5^2 + y_6^2),$$

$$\dot{y}_6 = -\omega(0.1 - \sigma y_2)y_5 + y_6 - y_6(y_5^2 + y_6^2),$$

where $\delta = 1 + \beta\cos^2 y_1$. Details of the full derivation of the continuum expansion can be found in Ref. [41]. Notice that the limit cycle is modeled by the last two equations. The frequency contains a feedback modulation term, representing the interaction of the pendulum and rod displacement with the periodic driver. The coupling is now bidirectional. As modeled, the truncated rod-beam system is autonomous. For our computations here, we use the parameters $\beta = 1$, $\zeta_1 = 0.01$, $\zeta = 0.01$, $\alpha = 1.8$, $\mu = 0.0625$, $\omega = 1.9527$, and $\sigma = 0.0001$. Here the relatively small value of σ indicates a small variation in the frequency of the driving term.

In the deterministic case, there is a chaotic attractor with one positive Lyapunov exponent. With additive noise of amplitude D, a nearby chaotic saddle is excited and the potential number of unstable dimensions is increased from one to two. This can be seen by the number of positive Lyapunov exponents. Figure 22(a) shows the six Lyapunov exponents for the pendulum model vs the noise amplitude. The system becomes high-dimensionally chaotic with two positive Lyapunov exponents for $D > D_c$, where $D_c \approx 10^{-0.18} \approx 0.66$. Notice that, for $D < D_c$, the second largest exponent represents the neutral direction. Figure 22(b) shows the scaling of this exponent with the noise variation on a logarithmic

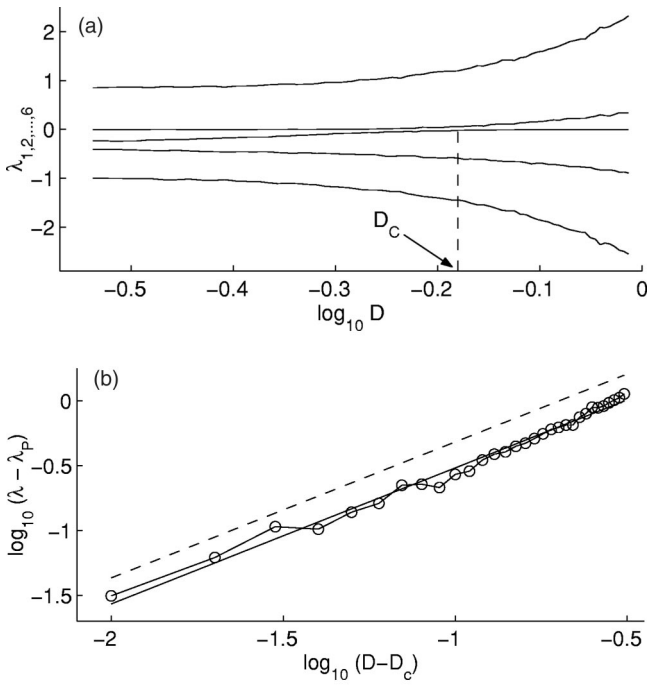

FIG. 22. (a) The Lyapunov exponents for the pendulum model vs the noise amplitude D. The critical noise amplitude for transition to high-dimensional noisy chaos is $D_c \approx 10^{-0.18}$. (b) The algebraic scaling of the noise-induced positive Lyapunov exponent with noise variation. The scaling exponent is close to unity, in agreement with our prediction.

scale. The scaling is apparently algebraic with the exponent 1.05 ± 0.04, which is close to unity. This example, together with others in Sec. IV, thus illustrates that our predicted scaling of the noise-induced positive Lyapunov exponent holds not only for low-dimensional chaos with one positive exponent but also for high-dimensional noisy chaos with multiple positive exponents.

B. Nonautonomous systems

Nonautonomous systems may also exhibit noise-induced chaos. The difference between autonomous and nonautonomous systems in terms of the Lyapunov exponents is that for the latter, there is always a zero Lyapunov exponent associated with the time axis, regardless of the noise level, as one can regard the time as an independent variable to convert the system into an autonomous one. For nonautonomous system under additive noise, the general observation is that the maximal Lyapunov exponent tends to increase as noise is increased through a critical value. Remarkably, this increase obeys the same algebraic scaling law as in autonomous systems.

As an illustrative example, we consider the following modified susceptible-infected model (MSI) arising in epidemiology [9,40]:

$$S'(t) = \mu - \mu S(t) - \beta(t) I(t) S(t),$$
$$I'(t) = \left(\frac{\alpha}{\mu + \gamma} \right) \beta(t) I(t) S(t) - (\mu + \alpha) I(t), \tag{46}$$

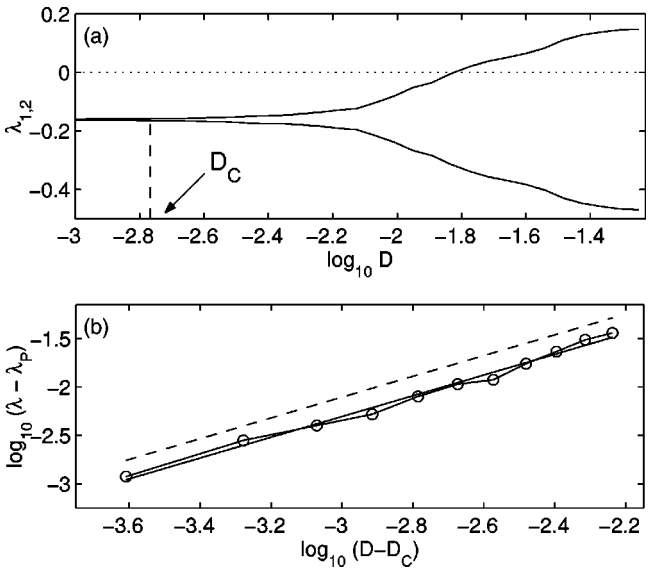

FIG. 23. (a) The Lyapunov exponents λ for the MSI model vs the standard deviation of the noise D. The critical noise amplitude is $D_c \approx 10^{-2.77}$. (b) The algebraic scaling between $\lambda - \lambda_P$ and $D - D_c$. The scaling exponent is 1.07 ± 0.05.

with $\beta(t) = \beta_0(1 + \delta \cos 2\pi t)$. In [9,40], this model was studied under additive noise. It was shown that for sufficiently strong noise, the dynamics of the system can be transformed from regular periodic cycles to stochastic chaos. In the deterministic case with parameter values at $\mu = 0.02$, $\alpha = 1/0.0279$, $\gamma = 100$, $\beta_0 = 1575$, and $\delta = 0.095$, there exist two stable periodic orbits, two unstable periodic orbits, and a partially formed heteroclinic orbit. There is no periodic window structure in the parameter space but instead, the noise essentially completes the near-heteroclinic tangencies to create noise-induced intermittency. The two stable periodic orbits and the stochastic chaotic saddle between them form a single connected dynamical invariant set, which has a positive Lyapunov exponent. The exponent appears to obey the algebraic scaling law.

Numerically, we observe that with additive noise, the second Lyapunov exponent is decreased. For large noise, the system becomes chaotic with one positive exponent and another negative Lyapunov exponent. (Note that the third Lyapunov exponent is not effected by noise and is always zero because it represents time.) Figure 23 shows the two nontrivial Lyapunov exponents vs the noise amplitude, where we observe that $\lambda_1 \approx \lambda_P$ for $D < D_c$ and starts to increase for $D > D_c$. The critical noise amplitude is estimated to be $D_c \approx 10^{-2.77} \approx 0.0017$. Figure 23(b) shows $\lambda - \lambda_P$ versus $D - D_c$ on a logarithmic scale, which appears to be linear. A least-squares fit gives the following estimate of the algebraic scaling exponent: 1.07 ± 0.05, which is close to unity.

VII. DISCUSSION

The interplay between deterministic chaos and noise has been a topic of continuous interest [1–9,13] as it is fundamental to both nonlinear dynamics and statistical physics.

While both noise and chaos signify random behavior in the system dynamics, their meaning and consequences are different. Chaos is characterized by a sensitive dependence on initial conditions, but a noisy system is not necessarily chaotic. There are, however, circumstances under which noise can induce chaos, a phenomenon that has long been recognized [1–9]. A common situation is where the system has the potential to become chaotic or it is already transiently chaotic. In such a case, as the noise amplitude is increased, the system can develop an attractor that emulates chaos. The characteristic features of the transition to chaos are the focus of this paper. Our main contributions are the following: (1) we find that the dynamics of noisy chaos is typically severely nonhyperbolic as it is associated with unstable dimension variability, (2) as a result of this nonhyperbolicity, for continuous-time physical systems described by differential equations, the topology of a noisy chaotic flow is fundamentally different from those of the deterministic flows (chaotic or nonchaotic) or of noisy nonchaotic flows in that there is no neutral direction associated with noisy chaos; and (3) we have established a universal scaling law associated with the largest Lyapunov exponent about the transition to noisy chaos.

Although our work is theoretical, some applied situations where our results may be relevant are the following. (1) It has been suggested that pathological destruction of chaotic behavior may induce some types of brain seizures [42] and heart failures [43]. In vital physiological systems chaotic dynamics can in fact be considered as ''normal'' [44]. Bifurcations to periodic behavior are viewed as a pathophysiological loss of the range of adaptive possibilities [45]. In these situations the presence of noise can be advantageous as it can help induce or restore chaos. (2) Maintaining chaos can be critical for industrial applications such as fluid mixing [46]. Noise can again be quite desirable. (3) There are applications where one wishes to induce chaos to disable systems such as electronic circuits, which can possibly be achieved by noisy perturbations. A good understanding of how a nonlinear system can emulate chaotic behavior in response to noise is clearly essential for designing the perturbations.

ACKNOWLEDGMENTS

Z.L. and Y.C.L. are supported by the AFOSR under Grant No. F49620-98-1-0400 and by the NSF under Grant No. PHY-9996454. I.B. was supported by the Office of Naval Research (ONR). L.B. was supported by the ONR under Grant No. N00173-01-1-G911.

[1] J. P. Crutchfield and B. A. Huberman, Phys. Lett. A **77**, 407 (1980); J. P. Crutchfield, J. D. Farmer, and B. A. Huberman, Phys. Rep. **92**, 45 (1982).

[2] J. M. Deutsch, Phys. Rev. Lett. **52**, 1230 (1984); J. Phys. A **18**, 1449 (1985).

[3] J. Rössler, M. Kiwi, B. Hess, and M. Markus, Phys. Rev. A **39**, 5954 (1989).

[4] J. M. Deutsch and G. Paladin, Phys. Rev. Lett. **62**, 695 (1989).

[5] F. Ladrappier and L.-S. Young, Commun. Math. Phys. **117**, 529 (1989).

[6] L. Yu, E. Ott, and Q. Chen, Physica D **53**, 102 (1992).

[7] J. B. Gao, S. K. Hwang, and J. M. Liu, Phys. Rev. Lett. **82**, 1132 (1999); S. K. Hwang, J. B. Gao, and J. M. Liu, Phys. Rev. E **61**, 5162 (2000).

[8] S. Rim, D.-U. Hwang, I. Kim, and C.-M. Kim, Phys. Rev. Lett. **85**, 2304 (2000).

[9] T. W. Carr, L. Billings, I. B. Schwartz, and I. Triandaf, Physica D **147**, 59 (2000); L. Billings and I. B. Schwartz, J. Math. Biol. **44**, 33 (2002).

[10] M. V. Jacobson, Commun. Math. Phys. **81**, 39 (1981).

[11] R. Abraham and S. Smale, Proc. Symp. Pure Math **14**, 5 (1970). In this paper, an ergodic invariant set in $\mathcal{R}^N$, with two saddle fixed points A and B, is constructed, and an argument is provided for the breakdown of shadowing of numerical trajectories, as a consequence of the unstable dimension variability. In particular, under the assumption of ergodicity, trajectories in the invariant set can spend arbitrarily long times near each point. Imagine a ball of initial conditions starting near A, which has an $(N-1)$-dimensional stable subspace. As the map is iterated, the ball of initial conditions is stretched into a thin curve along $W^u(A)$. The corresponding numerical trajectories lie within δ of the true trajectories given the roundoff error δ. Consider a phase space of $N=3$ dimensions. In the plane spanned by the two stable directions at A, all computer-generated trajectories lie in a circle of radius δ. The condition that both fixed points are embedded in an ergodic invariant set implies that some time later, trajectories near A visit a neighborhood of B. When the trajectories that started near A approach B, they begin to separate along the new unstable direction. Along this unstable direction, numerical and true trajectories separate from each other exponentially with time at a rate determined by the associated eigenvalue. The numerical trajectories can no longer be shadowed by the true trajectories at B.

[12] S. P. Dawson, C. Grebogi, T. Sauer, and J. A. Yorke, Phys. Rev. Lett. **73**, 1927 (1994); S. P. Dawson, *ibid.* **76**, 4348 (1996); P. Moresco and S. P. Dawson, Phys. Rev. E **55**, 5350 (1997); T. Sauer, C. Grebogi, and J. A. Yorke, Phys. Rev. Lett. **79**, 59 (1997); E. J. Kostelich, I. Kan, C. Grebogi, E. Ott, and J. A. Yorke, Physica D **109**, 81 (1997); Y.-C. Lai and C. Grebogi, Phys. Rev. Lett. **82**, 4803 (1999); E. Barreto, P. So, B. J. Gluckman, and S. J. Schiff, *ibid.* **84**, 1689 (2000); E. Barreto and P. So, *ibid.* **85**, 2490 (2000); H. Kantz, C. Grebogi, A. Prasad, Y.-C. Lai, and E. Sinde, Phys. Rev. E **65**, 026209 (2002).

[13] A. Maritan and J. Banavar, Phys. Rev. Lett. **72**, 1451 (1994); H. Herzel and J. Freund, Phys. Rev. E **52**, 3238 (1995); P. M. Gade and C. Basu, Phys. Lett. A **217**, 21 (1996); E. Sanchez, M. A. Matias, and V. Perez-Munuzuri, Phys. Rev. E **56**, 4068 (1997); C.-H. Lai and C. Zhou, Europhys. Lett. **43**, 376 (1998); C. Zhou and J. Kurths, Phys. Rev. E **65**, 040101 (2002).

[14] J. C. Sommerer and E. Ott, Science **259**, 335 (1993).
[15] Y.-C. Lai, Phys. Rev. E **53**, 57 (1996); Y.-C. Lai, U. Feudel, and C. Grebogi, *ibid.* **54**, 6070 (1996): T. Yalcinkaya and Y.-C. Lai, Phys. Rev. Lett. **77**, 5039 (1997).
[16] M. Harrison and Y.-C. Lai, Phys. Rev. E **59**, R3799 (1999); Int. J. Bifurcation Chaos Appl. Sci. Eng. **10**, 1471 (2000).
[17] The Lyapunov exponents are the time-averaged stretching or contracting rates of infinitesimal vectors along a typical trajectory in the phase space, regardless of whether the system is deterministic or stochastic.
[18] This consideration does not apply to nonautonomous systems for which there is always a neutral direction along the time axis and therefore always a zero Lyapunov exponent.
[19] Z. Liu, Y.-C. Lai, L. Billings, and I. B. Schwartz, Phys. Rev. Lett. **88**, 124101 (2002).
[20] In finite times, there can be deviations of the Lyapunov exponents of the noisy attractor from these of the periodic attractor. However, any deviations will vanish asymptotically, due to the averaging effect of the noise.
[21] C. Grebogi, E. Ott, and J. A. Yorke, Physica D **7**, 181 (1983); H. Kantz and P. Grassberger, *ibid.* **17**, 75 (1985).
[22] T. Tél, in *Directions in Chaos*, edited by Bai-lin Hao (World Scientific, Singapore, 1990), Vol. 3; in *STATPHYS 19*, edited by Bai-lin Hao (World Scientific, Singapore, 1996).
[23] C. Grebogi, E. Ott, and J. A. Yorke, Phys. Rev. A **37**, 1711 (1988).
[24] G.-H. Hsu, E. Ott, and C. Grebogi, Phys. Lett. A **127**, 199 (1988).
[25] H. E. Nusse and J. A. Yorke, Physica D **36**, 137 (1989).
[26] J. Jacobs, E. Ott, and C. Grebogi, Physica D **108**, 1 (1997).
[27] P. Grassberger, Phys. Lett. A **97**, 227 (1983); H. G. E. Hentschel and I. Procaccia, Physica D **8**, 435 (1983); P. Grassberger, Phys. Lett. A **107**, 101 (1985).
[28] T. C. Halsey, M. J. Jensen, L. P. Kadanoff, I. Procaccia, and B. I. Shraiman, Phys. Rev. A **33**, 1141 (1986).
[29] B. R. Hunt, E. Ott, and J. A. Yorke, Phys. Rev. E **54**, 4819 (1996).
[30] J. L. Kaplan and J. A. Yorke, in *Functional Differential Equations and Approximations of Fixed Points*, edited by H.-O. Peitgen and H.-O. Walter, Lecture Notes in Mathematics Vol. 730 (Springer, Berlin, 1979).
[31] R. M. May, *Stability and Complexity in Model Ecosystems* (Princeton University Press, Princeton, 1973).
[32] O. E. Rössler, Phys. Lett. A **71**, 155 (1979).
[33] P. E. Kloeden and E. Platen, *Numerical Solution of Stochastic Differential Equations* (Springer-Verlag, Berlin, 1992).
[34] E. Ott, *Chaos in Dynamical Systems* (Cambridge University Press, Cambridge, 1993), Chap. 9.
[35] E. N. Lorenz, J. Atmos. Sci. **20**, 130 (1963).
[36] In Ref. [47], a measure was introduced to quantify the degree of unstable dimension variability. This is the *contrast*, which is defined with respect to the infinite set of unstable periodic orbits. In particular, suppose there are two groups of orbits with one and two unstable directions; the contrast is

$$C_p = \left| \frac{\mu_2(p) - \mu_1(p)}{\mu_2(p) + \mu_1(p)} \right|,$$

where $\mu_{1,2}(p) \equiv \Sigma_{j=1}^{N_{1,2}(p)} e^{-\lambda_1^j(p)p}$, $N_1(p)$, and $N_2(p)$ are the numbers of periodic orbits of period p with one and two unstable directions, respectively, $\lambda_1^j(p)$ is the largest Lyapunov exponent of the jth periodic orbit of period p, and the factor $e^{-\lambda_1^j(p)p}$ approximates the natural measure associated with this orbit [23]. The quantities $\mu_{1,2}(p)$ are then the *weighted* numbers of period-p orbits with one and two unstable directions, respectively. When there is no unstable dimension variability, we have either $N_2(p)=0$ or $N_1(p)=0$, which yields $C_p=1$. The contrast C_p starts to decrease from one when unstable dimension variability occurs, and $C_p=0$ characterizes the situation where unstable dimension variability is most severe $[\mu_1(p)=\mu_2(p)]$. While both the topological rigidity introduced here and the contrast measure characterize the degree of unstable dimension variability, the former is relatively straightforward to compute because it does not involve the computation of unstable periodic orbits.
[37] For example, see H. Fujisaka and T. Yamada, Prog. Theor. Phys. **69**, 32 (1983); **72**, 885 (1984); **74**, 919 (1985); A. S. Pikovsky and P. Grassberger, J. Phys. A **24**, 4587 (1991); N. Platt, E. A. Spiegel, and C. Tresser, Phys. Rev. Lett. **70**, 279 (1993); Y.-C. Lai and C. Grebogi, Phys. Rev. E **52**, R3313 (1995); S. C. Venkataramani, T. M. Antonsen Jr., E. Ott, and J. C. Sommerer, Physica D **96**, 66 (1996); T. Yalcinkaya and Y.-C. Lai, Phys. Rev. Lett. **77**, 5039 (1997); Z. Liu and Y.-C. Lai, *ibid.* **86**, 4737 (2001).
[38] J. F. Heagy, N. Platt, and S. M. Hammel, Phys. Rev. E **49**, 1140 (1994); N. Platt, S. M. Hammel, and J. F. Heagy, Phys. Rev. Lett. **72**, 3498 (1994).
[39] D. Marthaler, D. Armbruster, Y.-C. Lai, and E. J. Kostelich, Phys. Rev. E **64**, 016220 (2001).
[40] L. Billings, E. Bollt, and I. B. Schwartz, Phys. Rev. Lett. **88**, 234101 (2002).
[41] I. T. Georgiou and I. B. Schwartz, SIAM (Soc. Ind. Appl. Math.) J. Appl. Math. **59**, 1178 (1999).
[42] S. J. Schiff, K. Jerger, D. H. Duong, T. Chang, M. L. Spano, and W. L. Ditto, Nature (London) **370**, 615 (1994).
[43] A. L. Goldberger, Ann. Biomed. Eng. **18**, 195 (1990); M. A. Woo, W. G. Stevenson, D. K. Moser, R. M. Harper, and R. Trelease, Am. Heart J. **123**, 704 (1992).
[44] C. A. Skarda and W. J. Freeman, Behav. Brain Sci. **10**, 161 (1987); W. J. Freeman, J. Theor. Biol. **171**, 13 (1994); Int. J. Intell. Syst. **10**, 71 (1995); Neural Netw. **13**, 11 (2000); J. Phys. (Paris) **94**, 303 (2000); W. J. Freeman, R. Kozma, and P. J. Werbos, BioSystems **59**, 109 (2001).
[45] W. Yang, M. Ding, A. J. Mandell, and E. Ott, Phys. Rev. E **51**, 102 (1995).
[46] J. M. Ottino, *The Kinematics of Mixing: Stretching, Chaos, and Transport* (Cambridge University Press, New York, 1989).
[47] Y.-C. Lai, Phys. Rev. E **59**, R3807 (1999).